Bayesian inference of maximum density in central collisions and contribution to compression energy between 40 to 100 MeV/nucleon

Results and comparisons with INDRA data and ELIE model

VALENTE Antonin (LPC CAEN) under the supervision of Olivier LOPEZ (LPC CAEN)
March 2025, FAZIA days

Outlines

1. Introduction
2. Motivations
3. Central Collisions : Neural Network approach for the reconstruction of the impact parameter
4. Inference of nucleon-nucleon cross section σ^*_{NN} in dense medium
5. Bayesian inference of the max density ρ_{max}
6. Systematic Results for ρ_{max}
7. Contribution of compression energy
8. Perspectives

1. Introduction

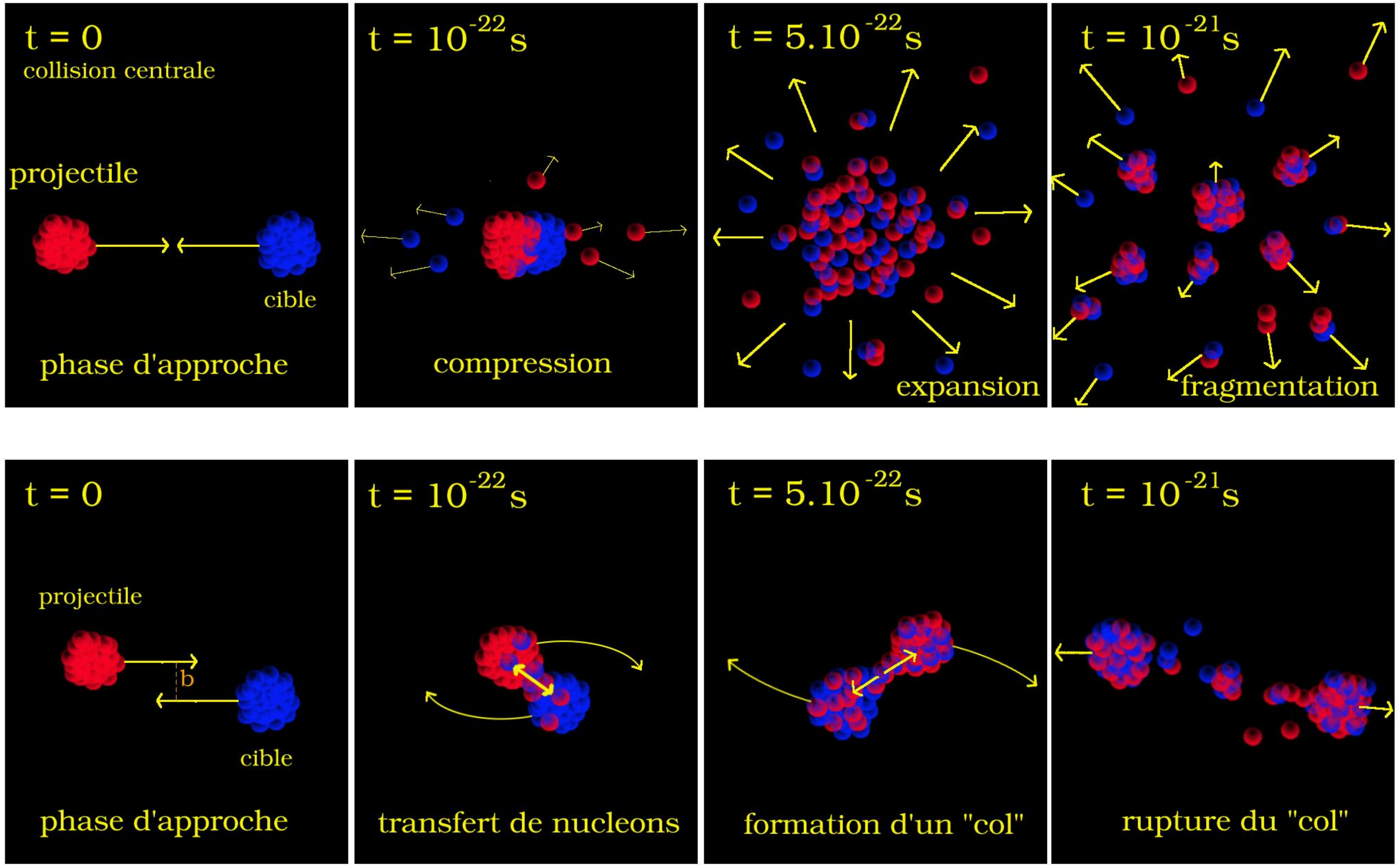

- Heavy ion collisions (HIC) around Fermi energy offer the possibility of compressing nuclear matter in order to explore densities far from saturation density ($\rho \sim 0.1 - 2\rho_0$).

- We can also heat the nuclear matter ($T \sim 1 - 10$ MeV) and perform nucleon exchange to measure isospin transfer ($N/Z \sim 1 - 1.5$).

- How can we do it? We use the INDRA-FAZIA device...

Experimental Setup

FAZIA Detector

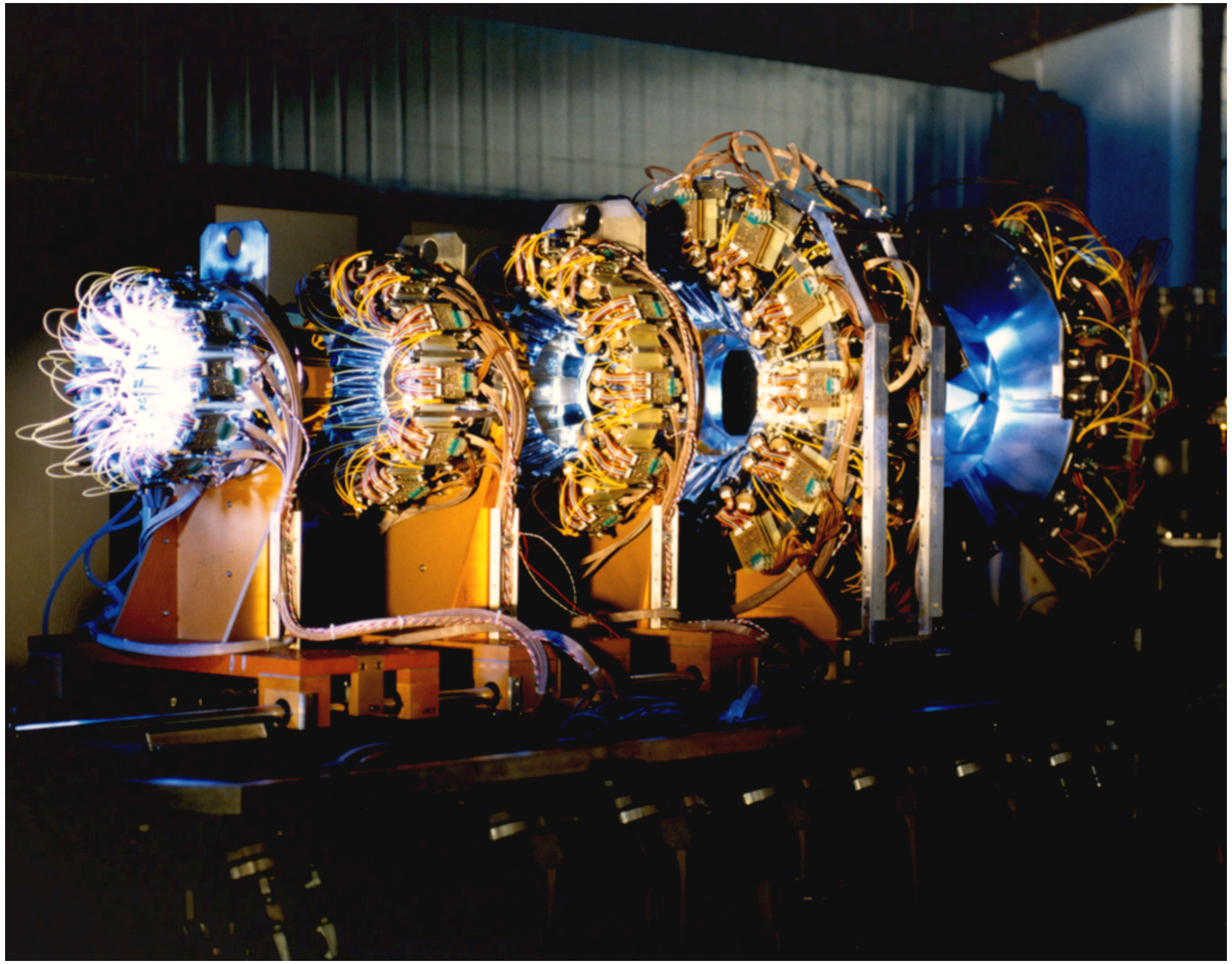

- INDRA is a light charged particle detector covering a wide solid angle of detection.

- INDRA measures backward angles.

- A beam of $^{58}Ni/^{58}Ni$ and $^{129}Xe/^{119}Sn$ imping a target over a range of energies from 32 to 90 MeV/nucleon.

- We can collect the charge (Z), the energy (E), the mass (A for $Z < 4$) and the angles (ϕ, θ) to rebuild the linear momentum ($\vec{p}$), the multiplicity (M), ...

- We can then proceed to construct global variables to characterize the equation of state (EOS)...

Equation of State

$$E(\delta, \rho) = E_{iso}(\rho) + E_{vec}(\rho)\delta^2 + \mathcal{O}(\delta^4)$$

With:

$$E_{iso}(\rho) = E_{sat} + \frac{K_{sat}}{2}\left(\frac{\rho - \rho_0}{3\rho_0}\right)^2 + \mathcal{O}(\rho^3)$$

$$E_{vec}(\rho) = E_{sym} + L_{sym}\left(\frac{\rho - \rho_0}{3\rho_0}\right) + \cdots$$

$$\cdots + \frac{K_{sym}}{2}\left(\frac{\rho - \rho_0}{3\rho_0}\right)^2 + \mathcal{O}(\rho^3)$$

- The equation of state (EOS) relates pressure, energy density and other thermodynamic properties of nuclear matter. The equation is Taylor expanded around ρ_0 and made of two parts: isoscalar and isovector.

- The first term (isoscalar) depends on density ρ. The second term (isovector) has isospin dependencies δ (isospin asymetry) and in density ρ.

- E_{sat} the saturation energy and K_{sat} is the curvature of the isoscalar energy component. E_{sym} is the symmetry energy, L_{sym} the slope, K_{sym} the curvature of the isovector part.

- Constraining these parameters is the objective of my thesis. This can be achieved using a Machine Learning approach...

2. Motivations

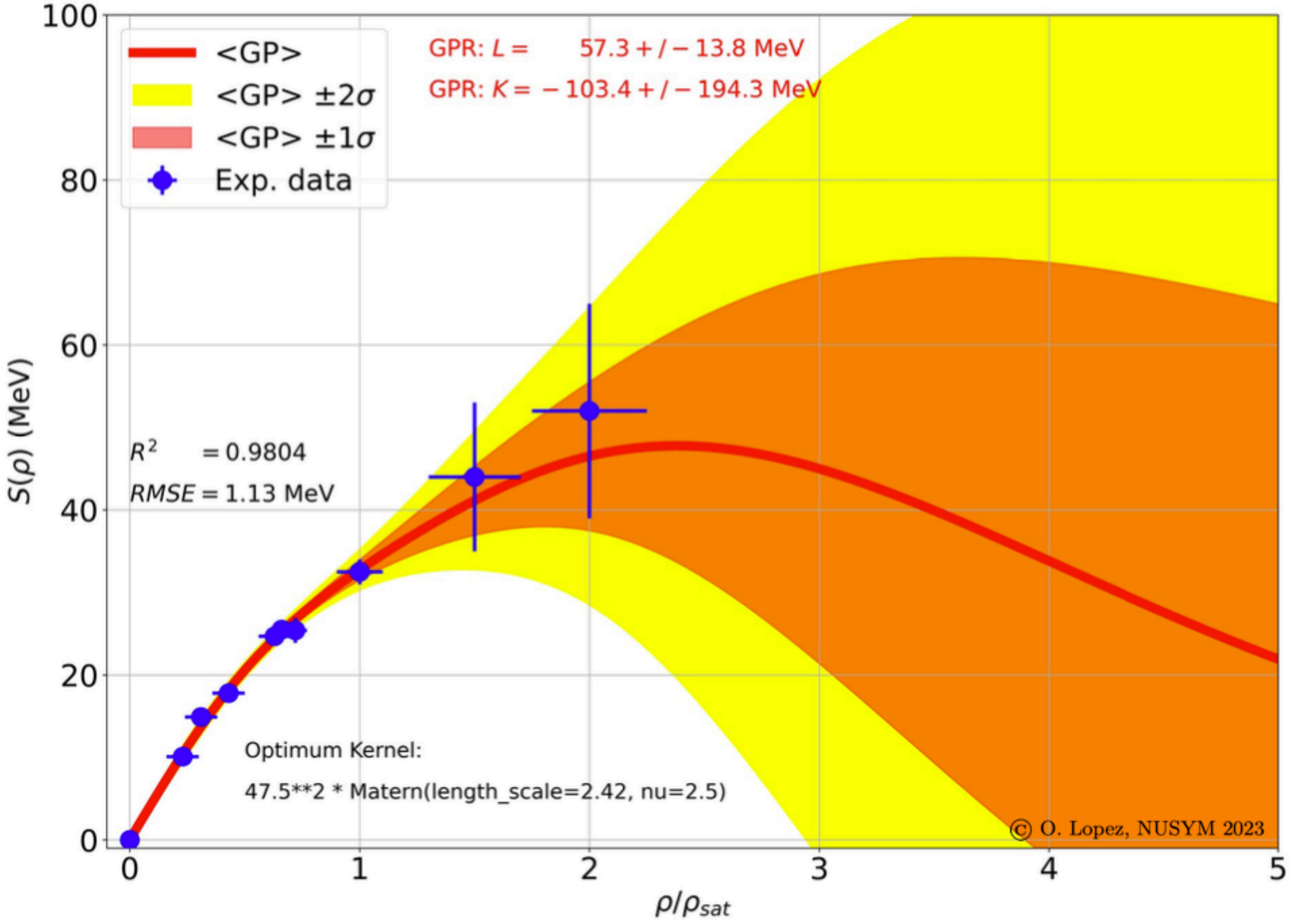

- For example, we can cite the work of O. Lopez. This is a gaussian emulation symmetry energy from the experimental data in the literature. (O. Lopez, NUSYM 2023)
- Symmetry energy $S(\rho)$, which is the energy cost per nucleon to go from symmetric matter (N=Z) of a nuclear system to a given baryonic density ρ to a system consisting purely of neutrons (N=A).
- The more the density range is explored, the better the constraint on the parameters L_{sym} and K_{sym}.
- The aim of my thesis is to use machine learning and Bayesian inference techniques on INDRA datasets in order to improve and constrain equation of state (EOS) parameters.

Nucleon-nucleon cross sections and the equation of state (EOS)

- To study the EOS we use Heavy Ion Collisions, those collisions must be calculated with a transport model which needs the value of the nucleon-nucleon cross section.

- Nucleon-nucleon (NN) cross sections σ^*_{NN} describe the fundamental interaction between two nucleons (protons or neutrons) in the atomic nucleus. They determine the probability of these particles colliding or scattering when they meet.

- By accurately modeling NN interactions from experimental scattering data, the energy and isospin contributions of the nuclear interaction in the medium can be determined.

- These energy contributions are used to construct the mean nuclear interaction potential. This mean potential is then used to solve the nuclear mean field equation and obtain the equation of state.

- Consequently, an accurate description of NN cross sections is crucial to correctly calculate the saturation properties of infinite nuclear matter (density, binding energy, symmetry energy, compressibility, etc.) predicted by the equation of state.

3. Central collisions : Neural Network approach to the impact parameter

Illustration of a Neural Network

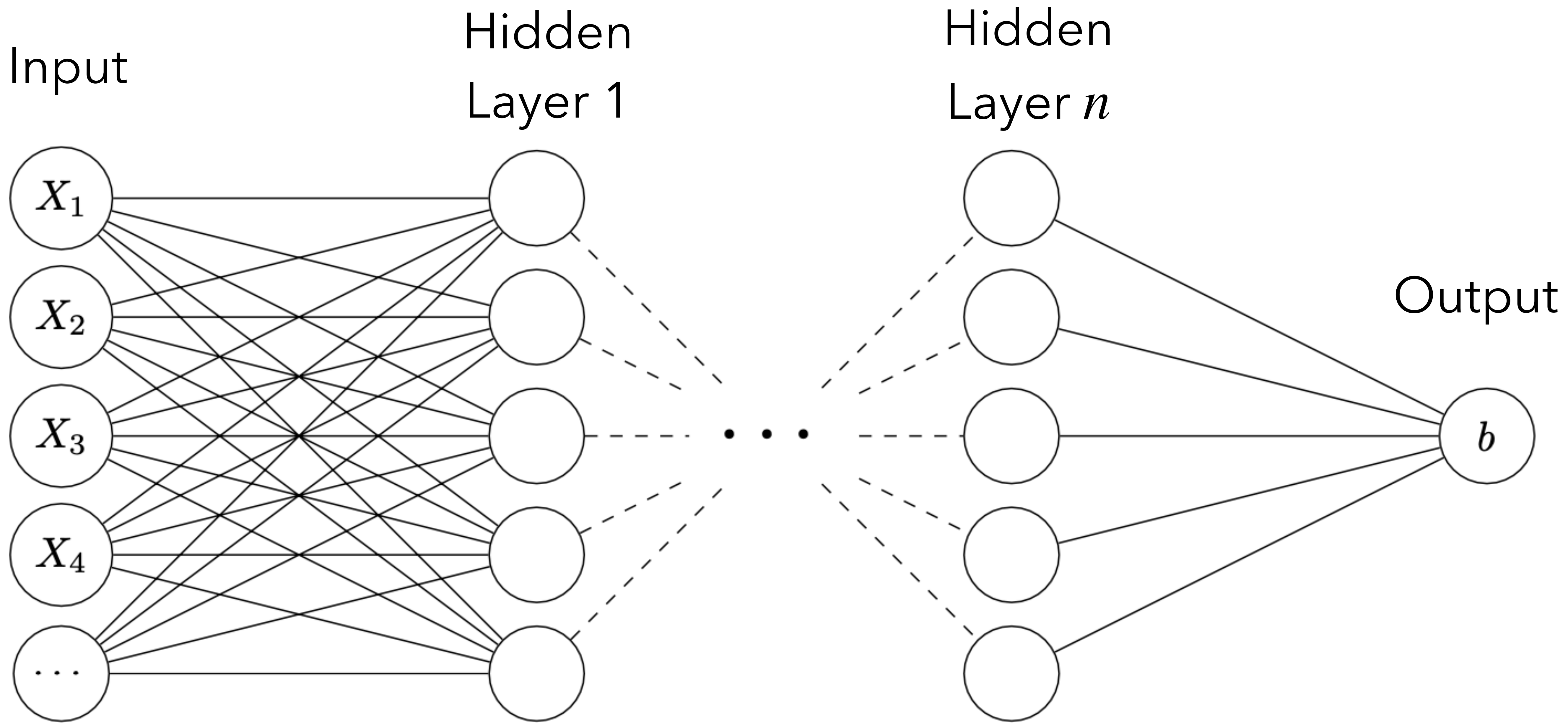

- The architecture is a neural network with 4 hidden layers, with 256, 128, 64 and 32 neurons respectively in this order.
- The selected activation function is EULU.
- The training dataset represents 80% and the test dataset 20%, with backpropagation and gradient descent for regression.
- The mean square error (MSE) is the estimator of the error to be minimized.

Impact parameter results

Correlation *HIPSE* & *ELIE* model

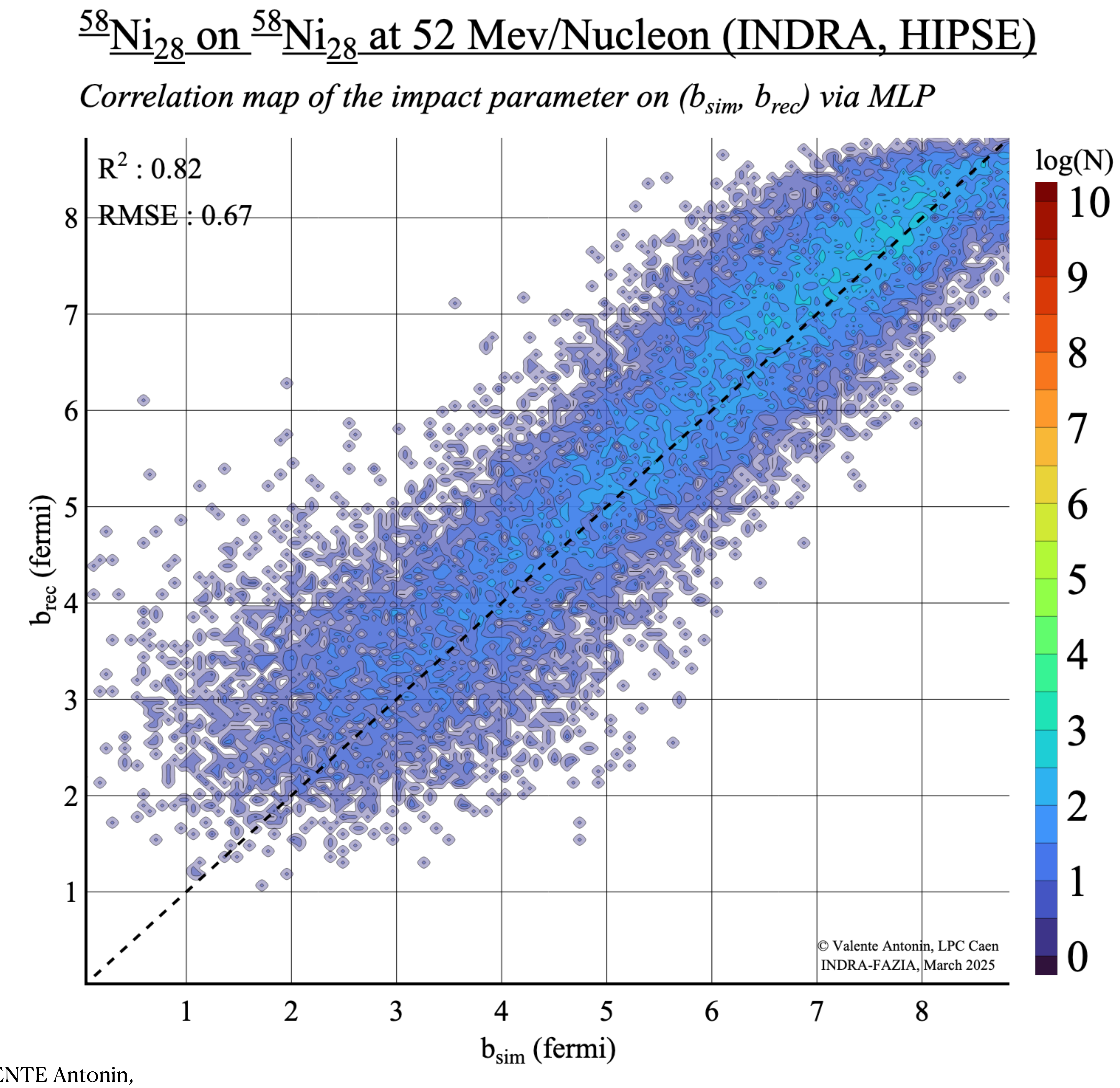

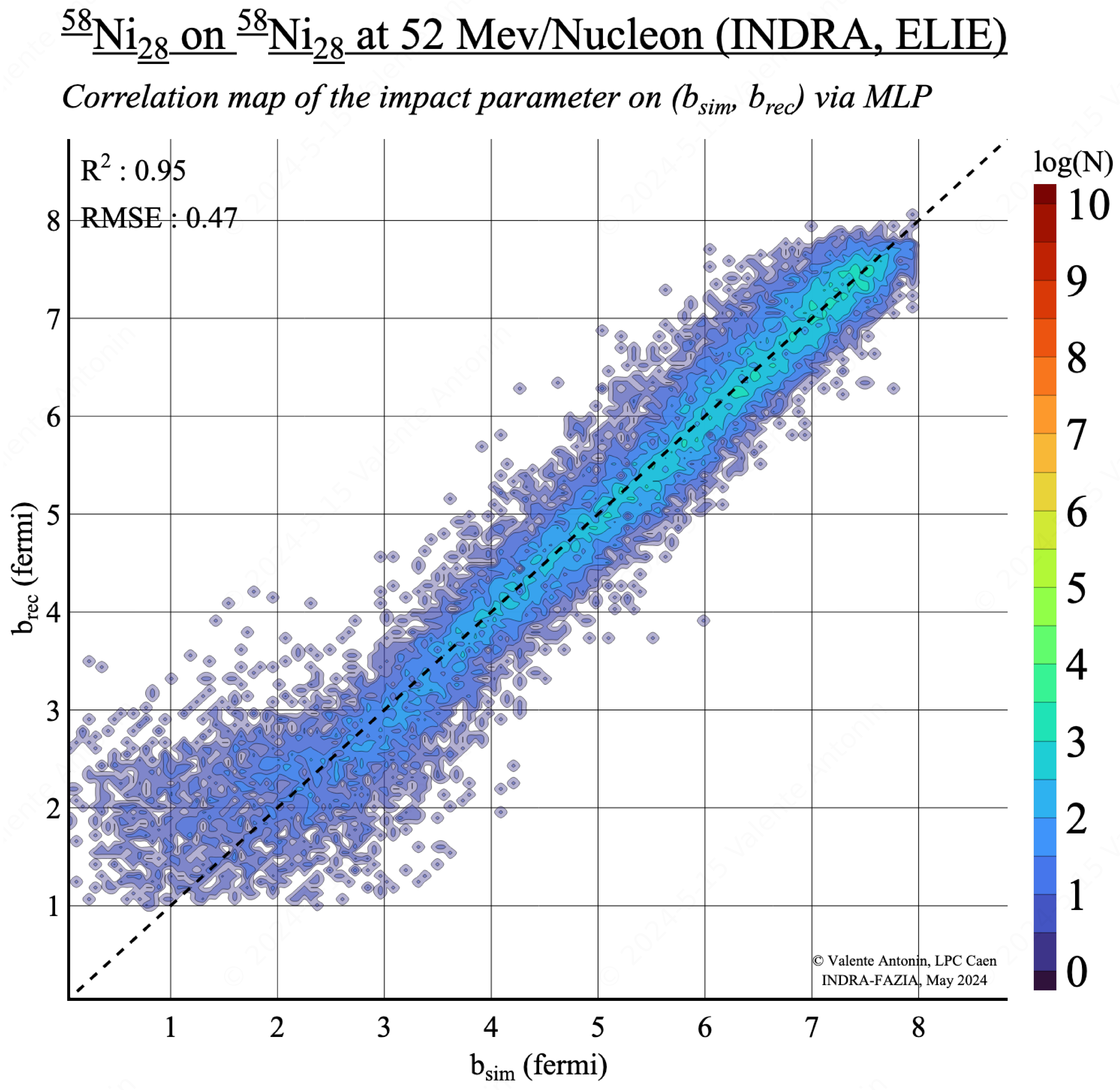

Charge vs. Parallel velocity of particles classified by centrality classes with impact parameter reconstructed on the experimental dataset

Central

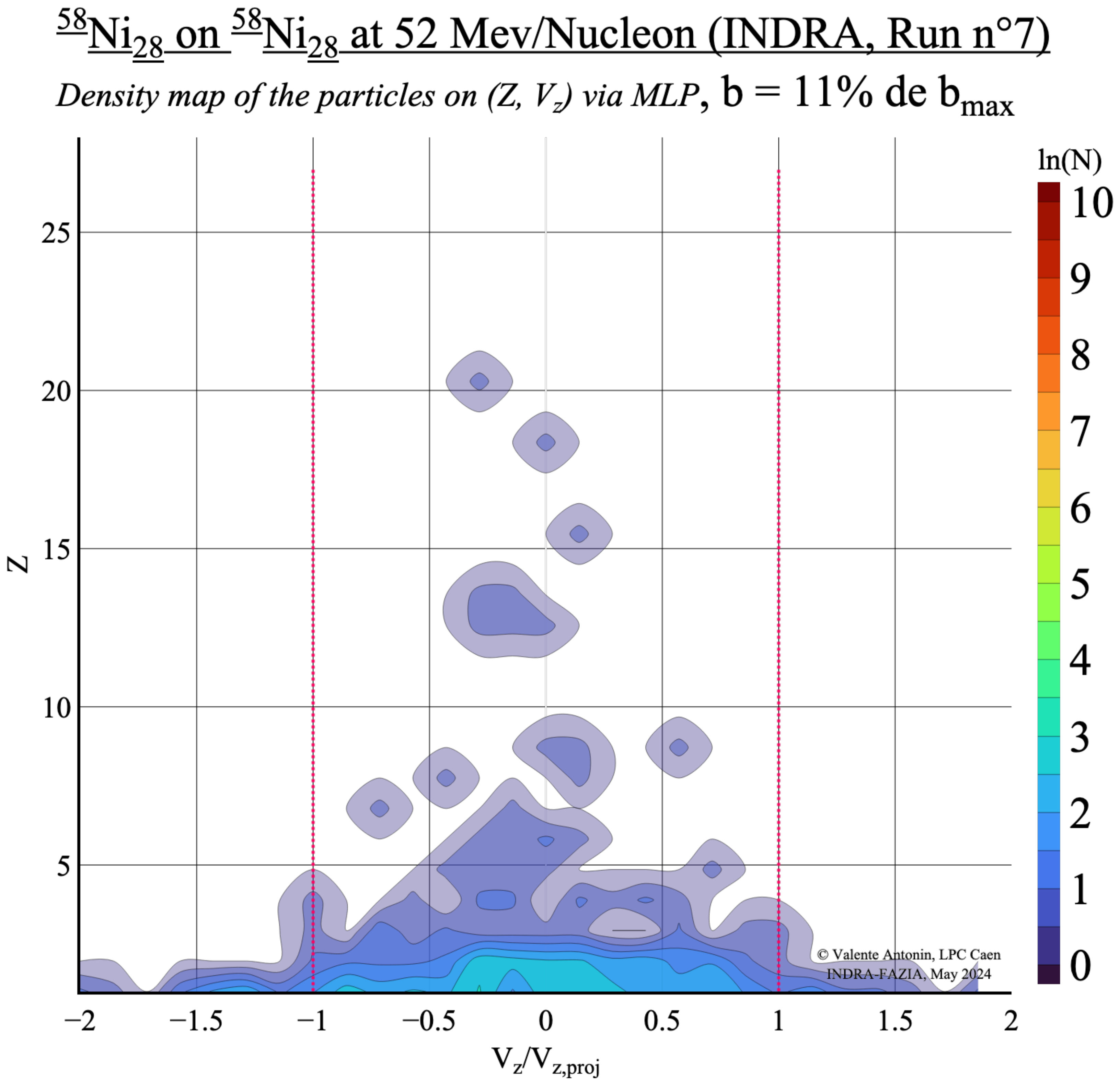

Semi-Central

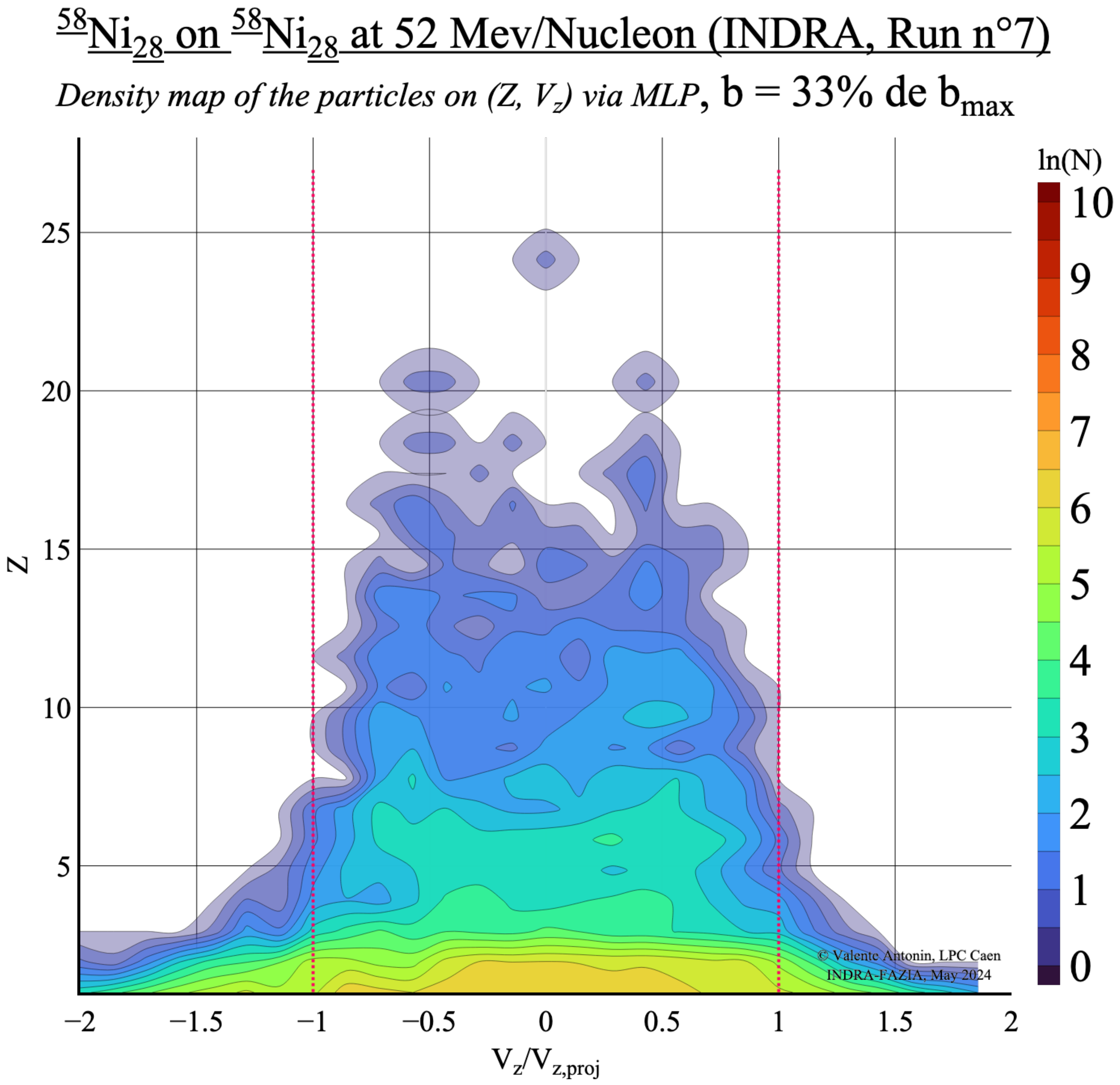

Intermediary

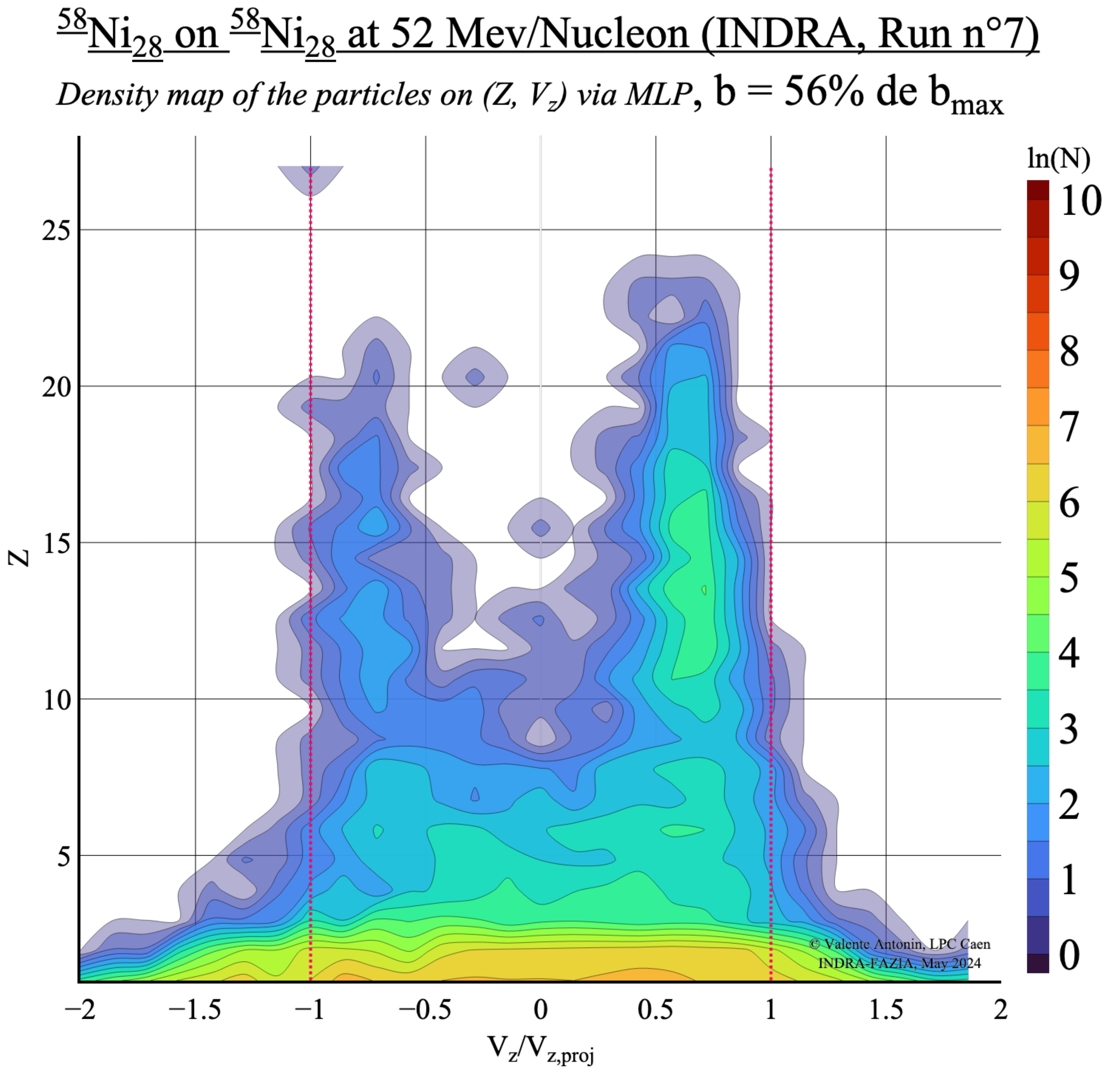

⚠️ The « b » values of each figure is an interval of the impact parameter distribution ⚠️

Semi-peripheral

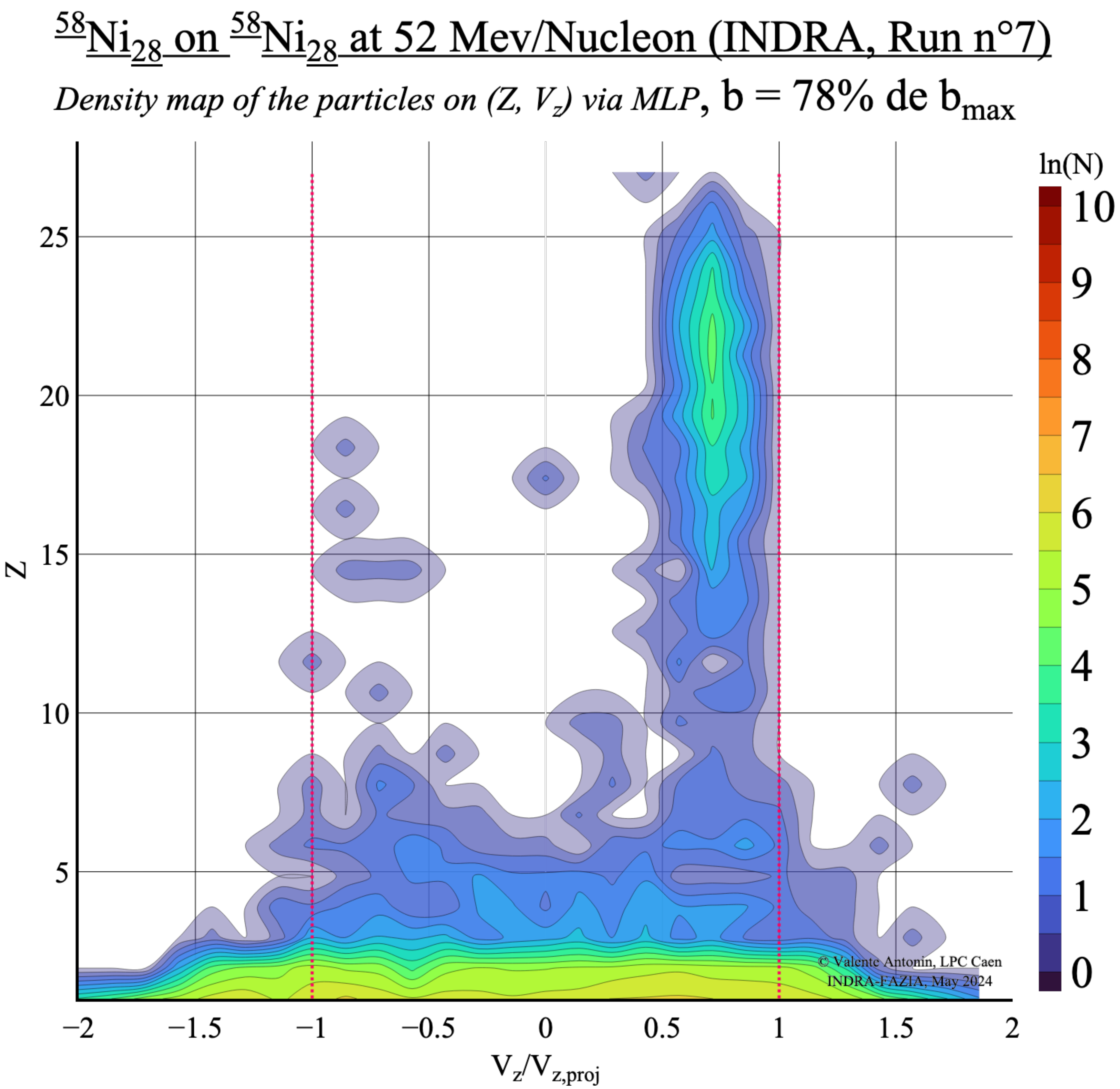

Peripheral

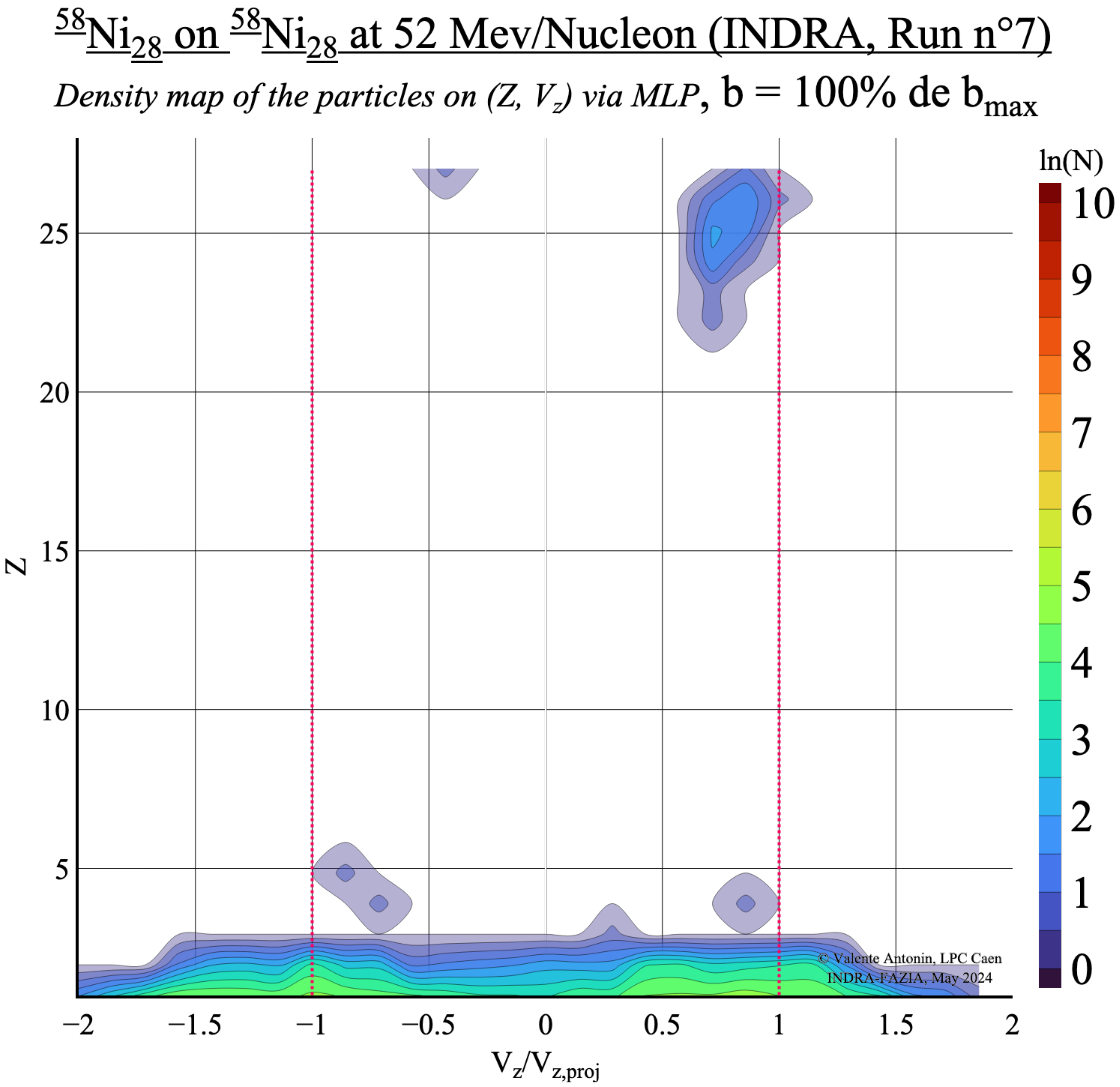

4. Inference for nucleon-nucleon cross section

We sample the NN cross-section with a uniform probability distribution (less informative distribution) during the simulation:

$$P(x) = \begin{cases} \frac{1}{\sigma_{max} - \sigma_{min}} & \text{if } x \in [\sigma_{min}, \sigma_{max}] \\ 0 & \text{if } x \notin [\sigma_{min}, \sigma_{max}] \end{cases}$$

We then divide the interval $\left[\sigma_{\mathrm{min}}; \sigma_{max}\right]$ into 20 bins and calculate a Kolmogorov probability for each bin.

The range explored is from 0 to 100 mb.

For the moment, the study is focused on the ELIE model, and we will do the same with HIPSE.

Results for σ_{nn}

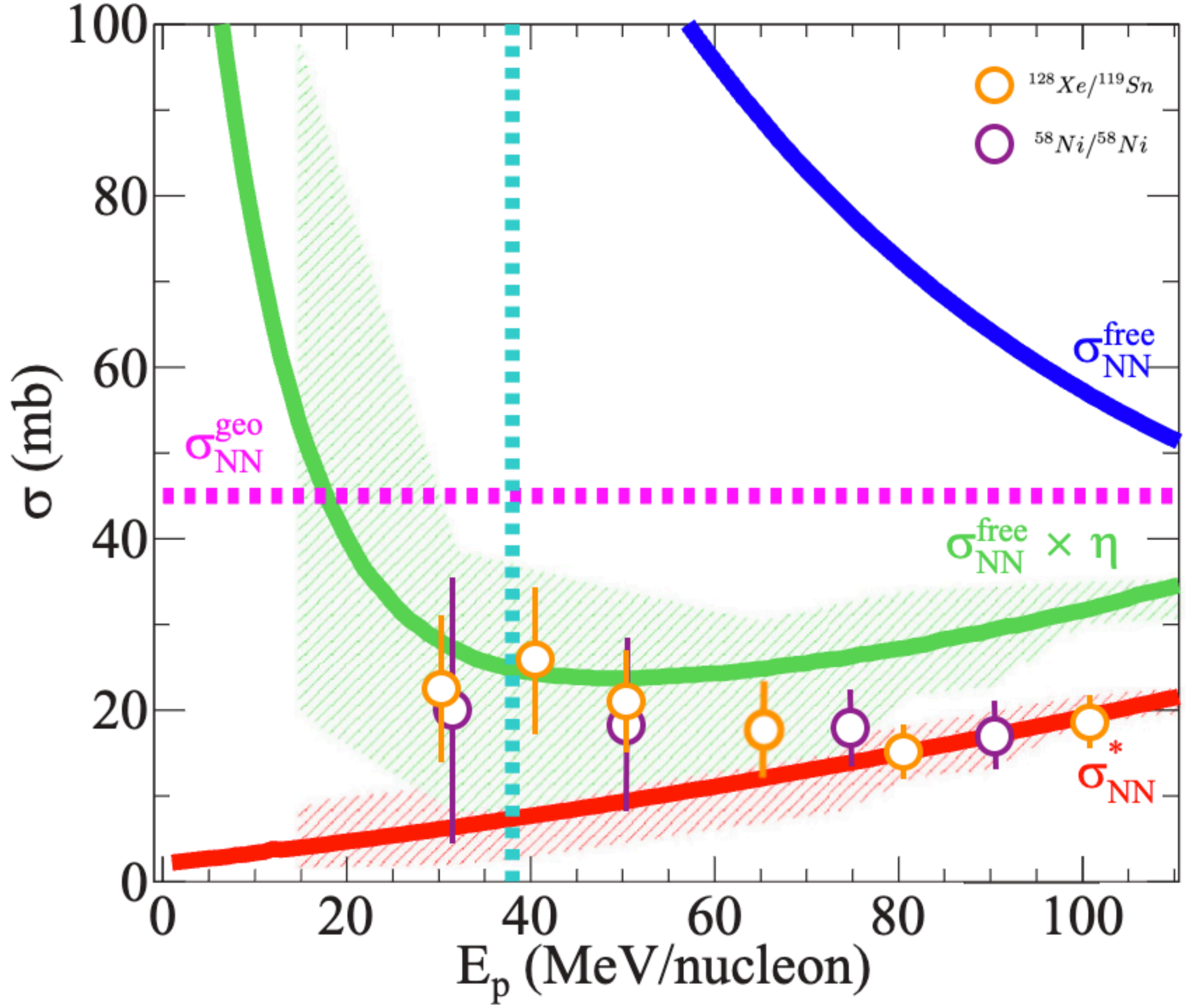

- The solid curves are from M. Henri et al (PRC 101, 064622 (2020)). The blue curve represents free nucleon-nucleon cross section, and the green curve represents the first curve corrected by a Pauli blocking effect. The red curve is the nucleon-nucleon cross section with in-medium effect proposed by D.D.S. Coupland et al. (PRC 84, 054603 (2011)).

- On this curve, I've displayed my Bayesian analysis results. The $^{58}Ni/^{58}Ni$ and $^{129}Xe/^{119}Sn$ are presented. These results are in good agreement with the in-medium effect on the effective cross-section for the upper energy range.

- For the lower range, uncertainties increase and we cannot conclude whether the effective cross-section is governed solely by the Pauli blocking effect or by a in-medium effect . We suspect that the ELIE model is not well suited to this energy range.

Summary for σ_{nn}

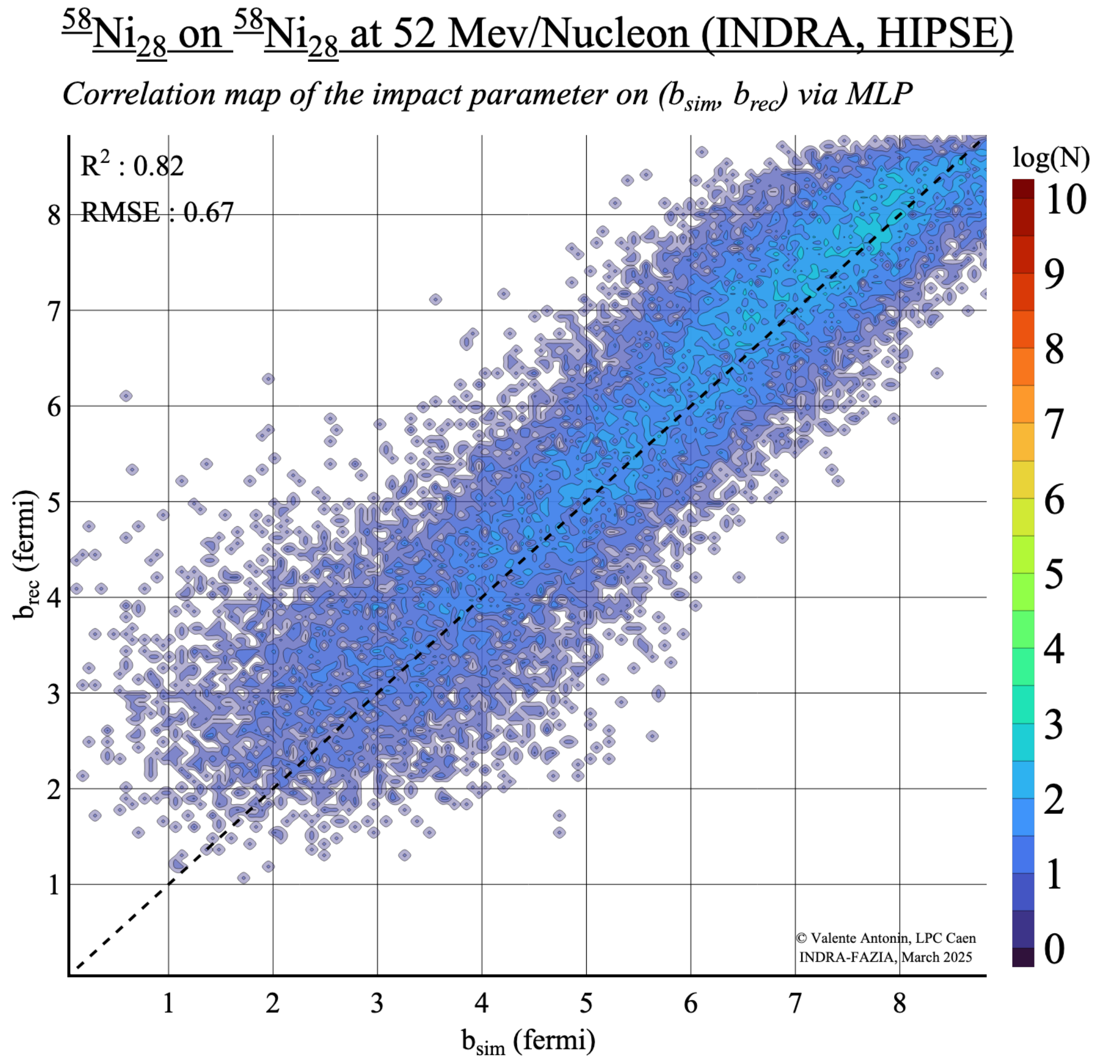

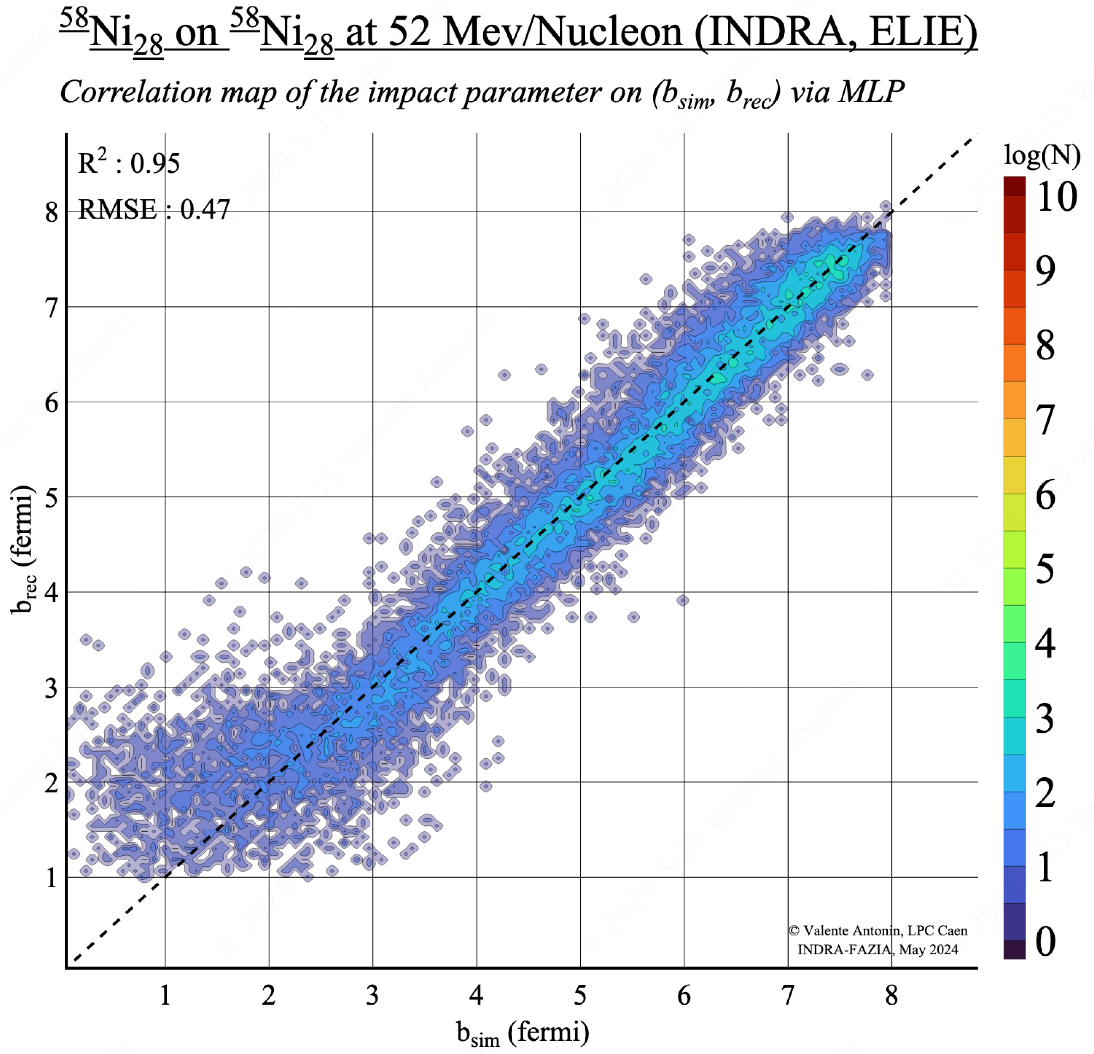

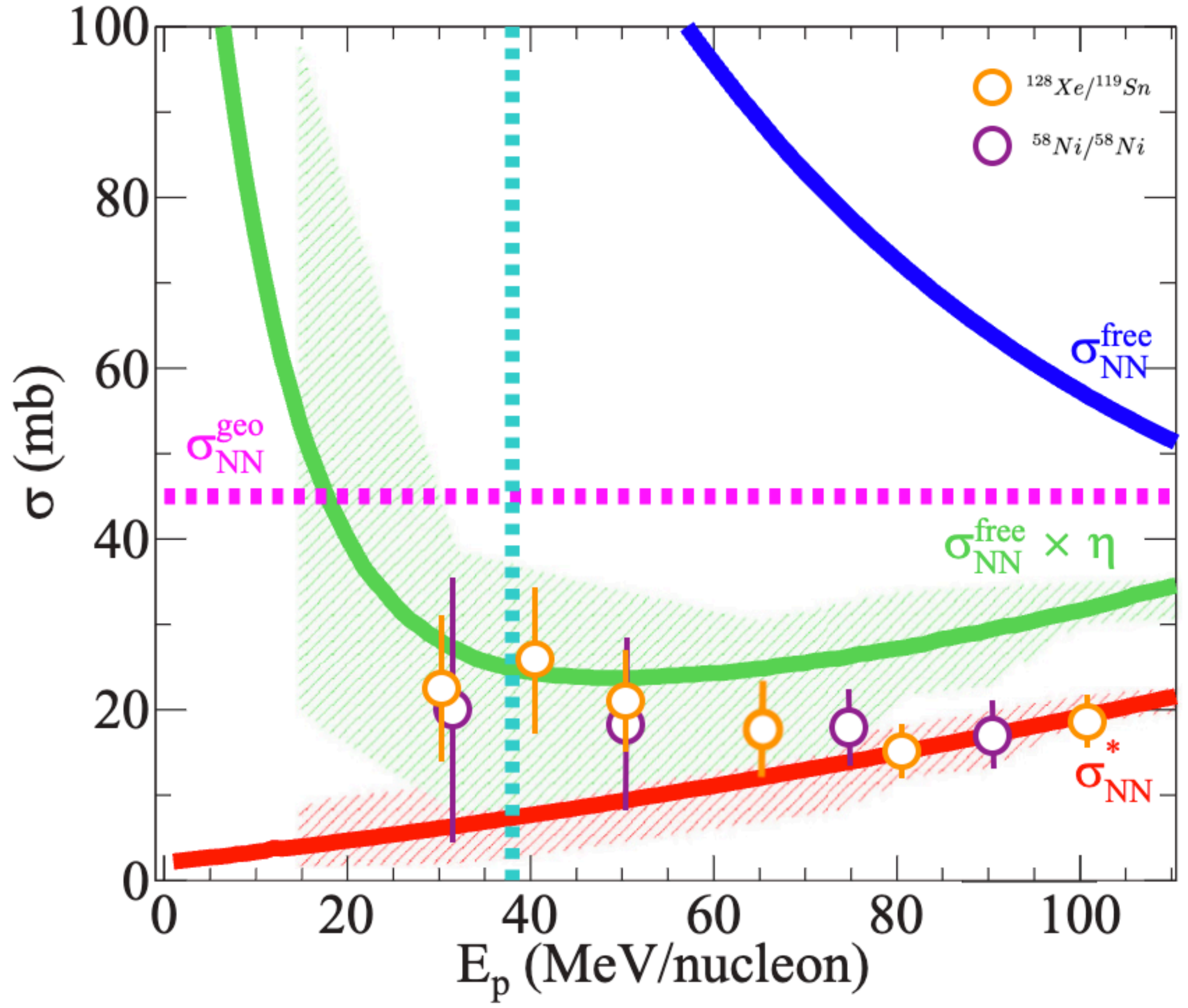

- Inference via machine learning on the impact parameter: selection of central and peripheral events. The impact parameter is inferred with an **error of less than 1 fermi**.
- Inference of the nucleon-nucleon cross section in dense medium with the ELIE model. The results show **a good agreement with M. Henri's results**, and we also provide **mean values and error bars based on experimental data**. To be continued with other systems.
- We will also pursue these inferences with density to determine the parameters of the equation of state (EOS)...

5. Bayesian inference of the maximal density ρ

We use an uniform distribution of the density as we did for the σ_{nn}.

This simulated distribution is then filtered and gives us the filtered *prior* for our analysis:

$$P_{prior}(\theta) \xrightarrow{\text{filtering}} P^{\star}_{prior}(\theta)$$

This eliminates events that are impossible to detect and to obtain a better quality *prior* for analysis.

We use the most central events

$b/b_{max} < 0.4$ **and "complete" events**

Bayes Theorem

Bayes' theorem is then used for this *prior*.

$$P_{posterior}(\theta|D) = \frac{P^{\star}_{prior}(D|\theta)P^{\star}_{prior}(\theta)}{P(D)}$$

where :

- $P(D)$, is the experimental distribution of a global observable D
- $P^{\star}_{prior}(D\,|\,\theta)$, is the simulated filtered distribution of an observable D given a parameter value θ.

Discretisation

By applying a numerical version of this theorem for a **sampling** j **of** D **(data)** and i **of** θ **(model parameter)** :

$$P_{posterior}(\theta_i|D_j) = \frac{P^{\star}_{prior}(D_j|\theta_i)P^{\star}_{prior}(\theta_i)}{P(D_j)}$$

The result is a density map $P_{posterior}(\theta_i \mid D_j)$.

In the density application here, we will test ρ for a sample of 50 bins and various observables D with the same sampling.

Bayesian inference for the density ρ_{max}

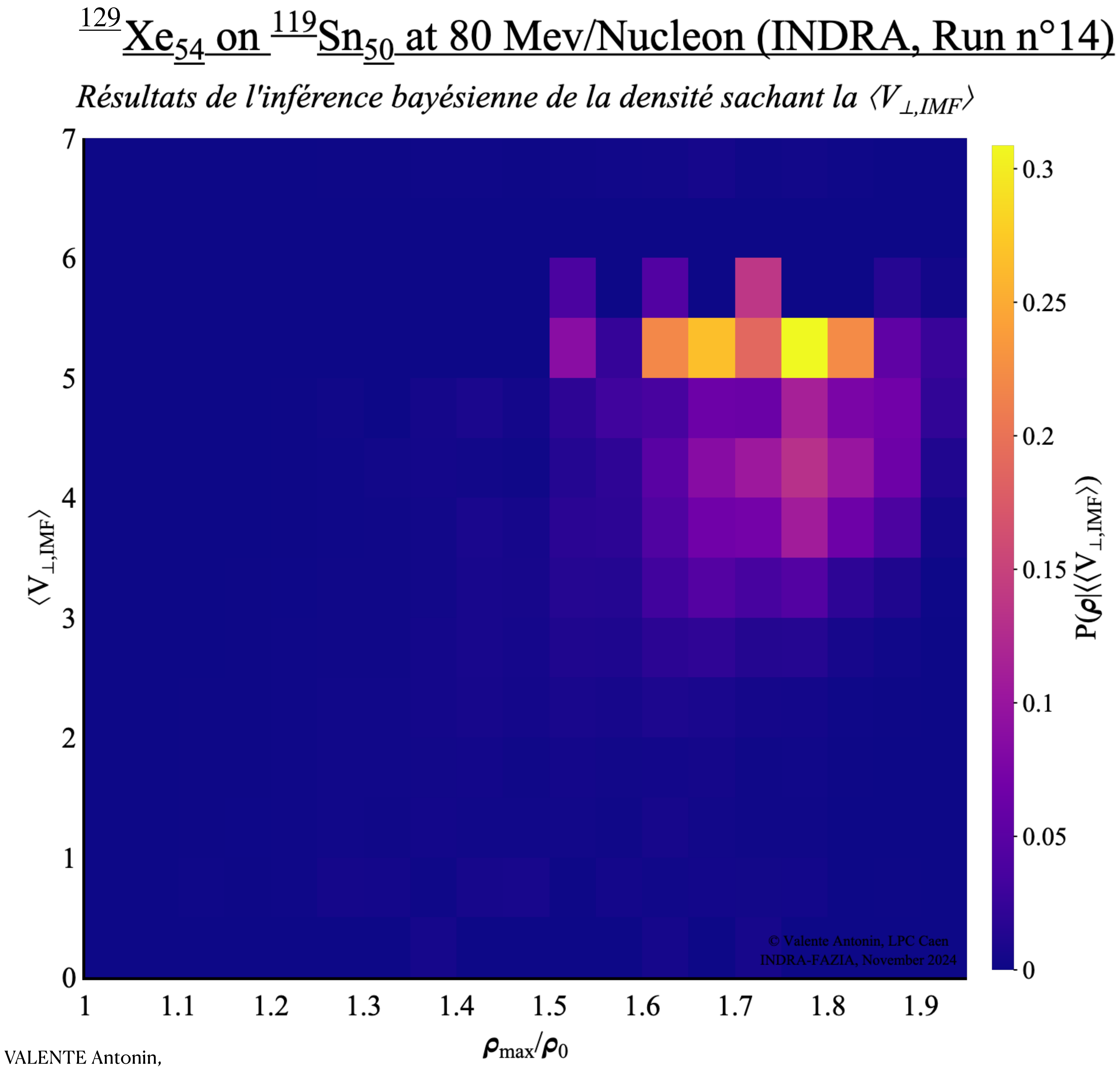

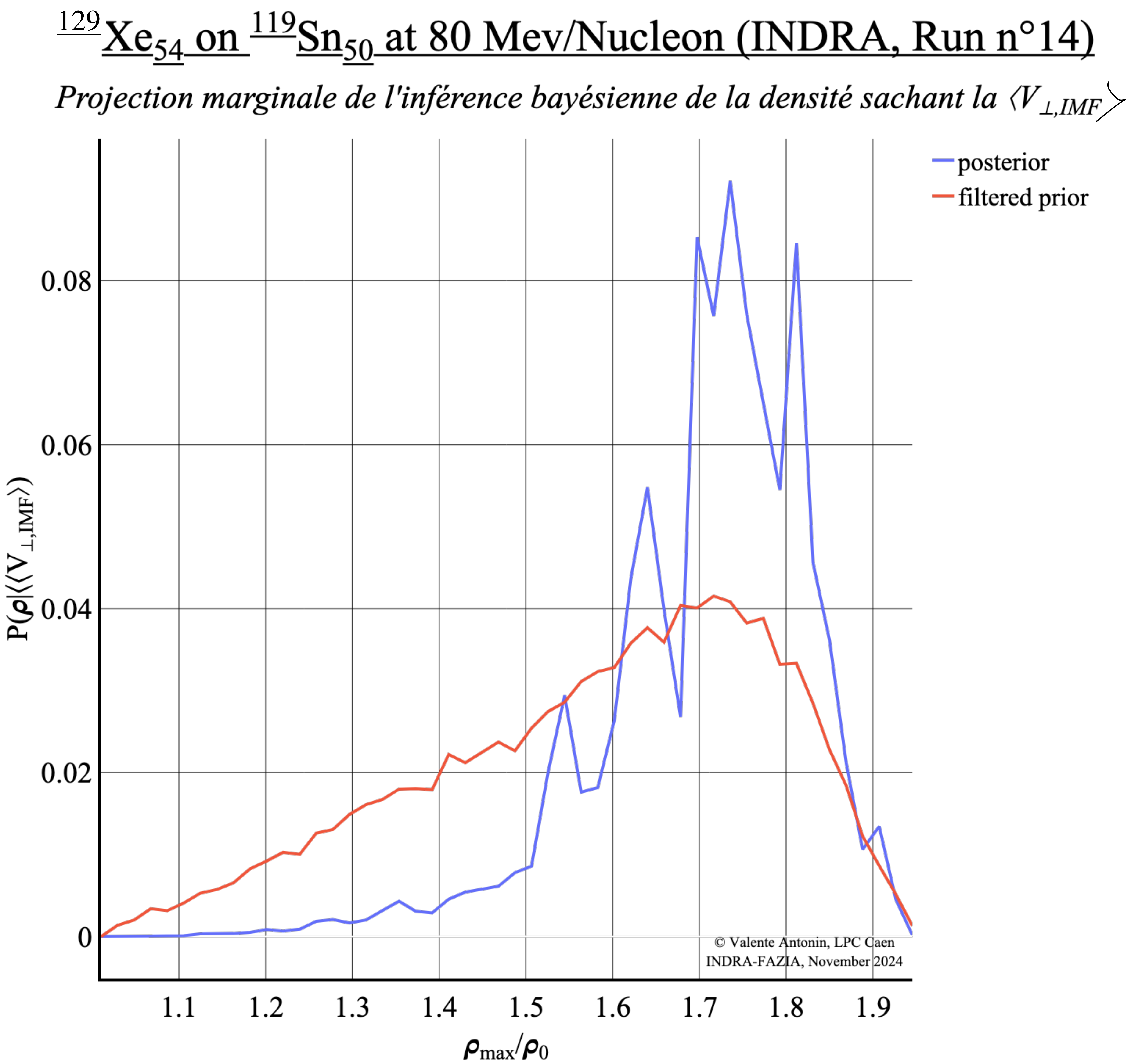

$^{129}Xe_{54}$ on $^{119}Sn_{50}$ at 80 Mev/Nucleon (INDRA, Run n°14)

Projection marginale de l'inférence bayésienne de la densité sachant la $\langle V_{\perp,IMF}$

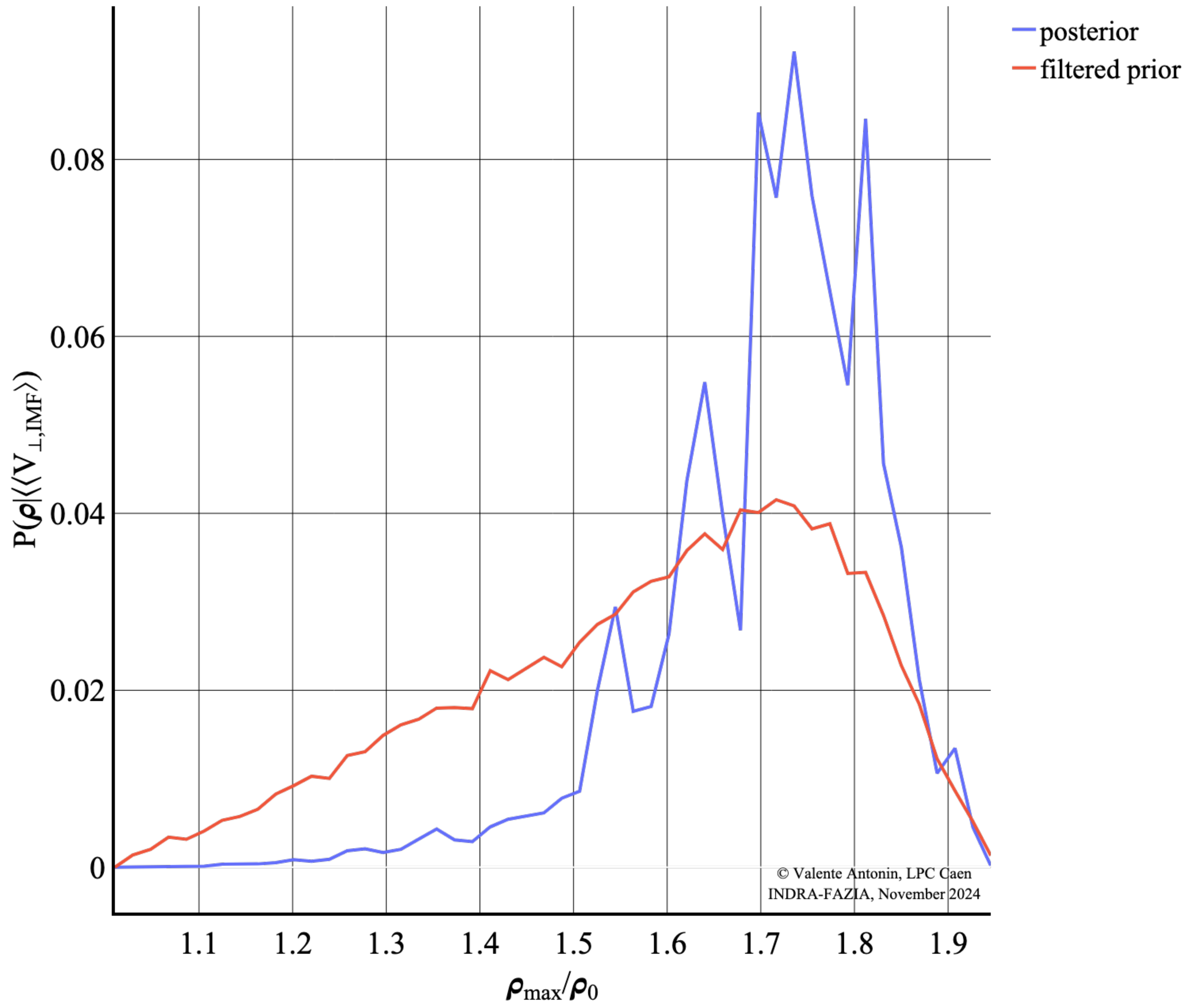

On the marginal projection in density of :

$$P_{posterior}(\theta_i|D_j)$$

We can have :

$$P_{posterior}(\theta_i)$$

This distribution can then be defined by the mean and the width:

$$\langle \rho_{max}/\rho_0 \rangle \pm \sigma_{\rho_{max}}$$

6. Systematics Results

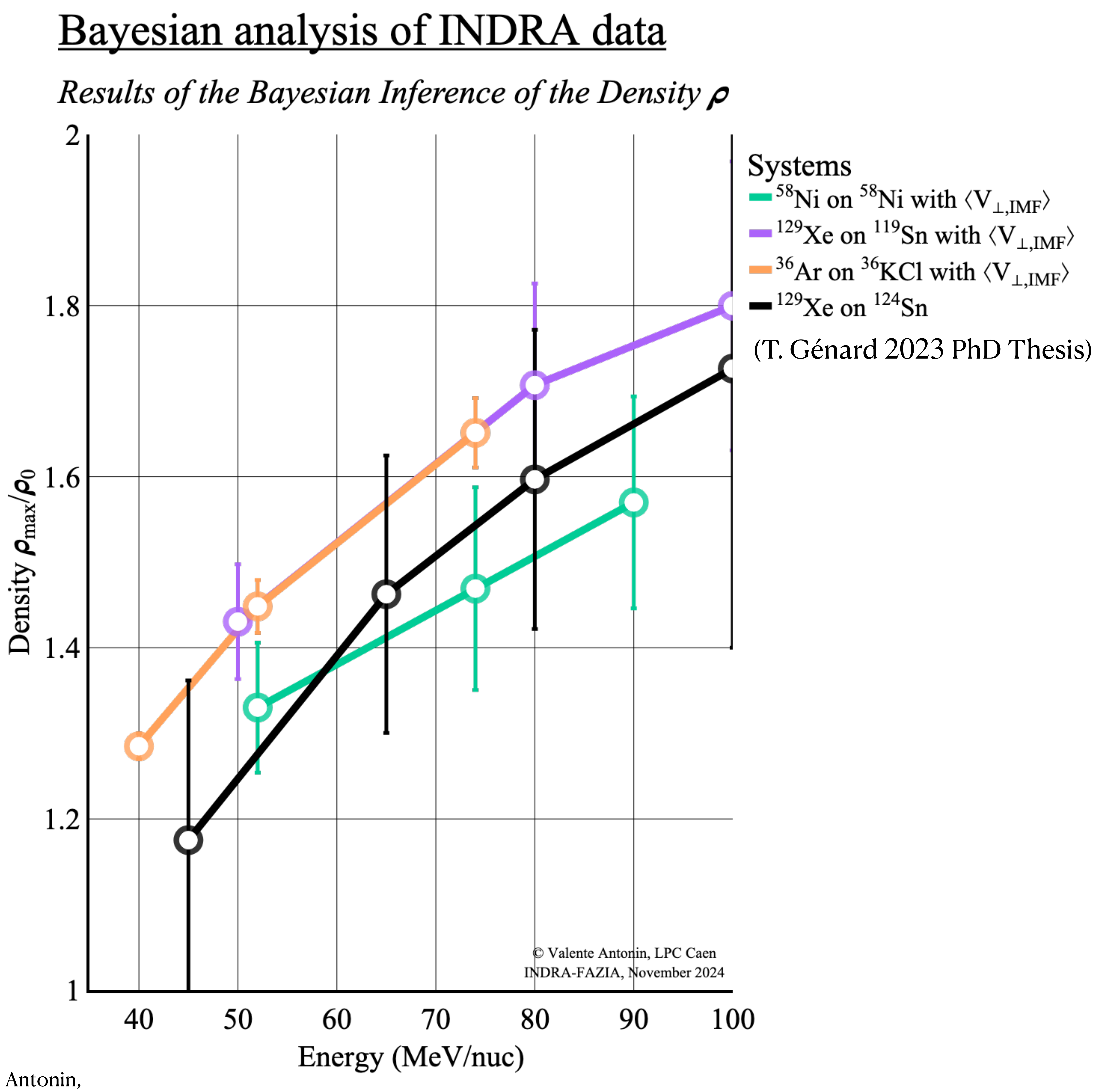

The most sensitive observable most in this work is the average transverse velocity of the IMFs $\langle V_{\perp,IMF} \rangle$ which was suggested by Dominique DURAND in a previous work using ELIE.

Summary for ρ_{max}

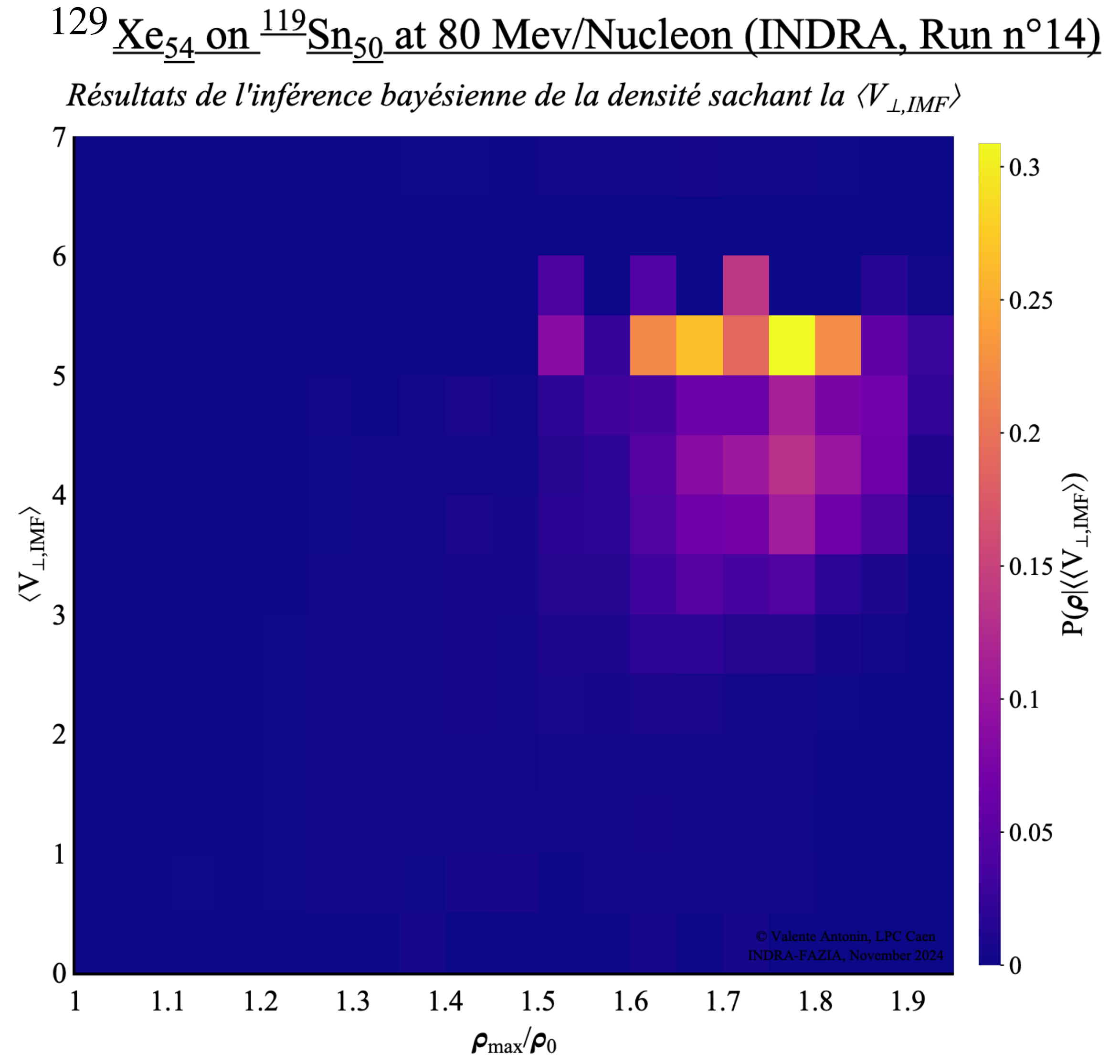

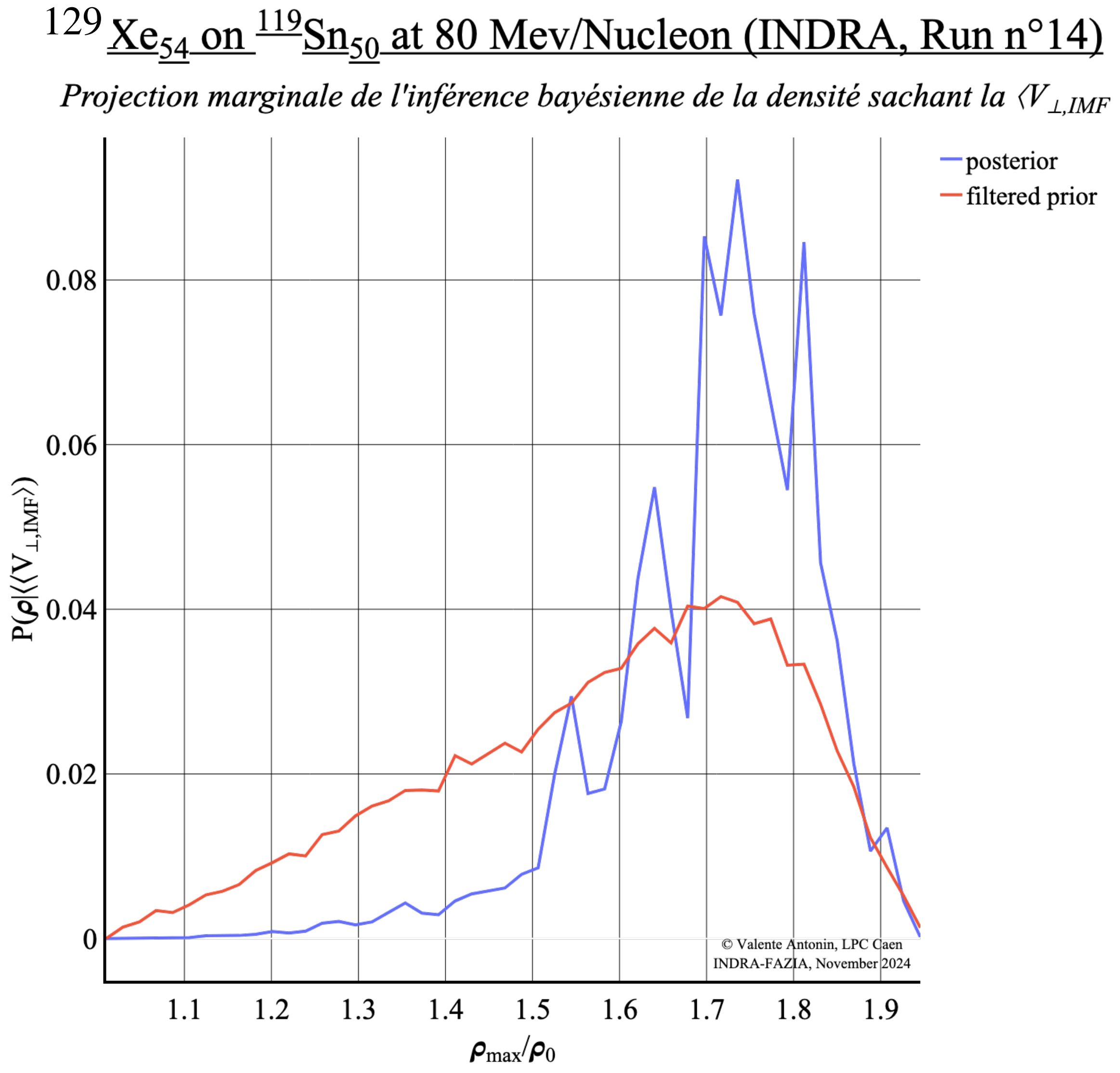

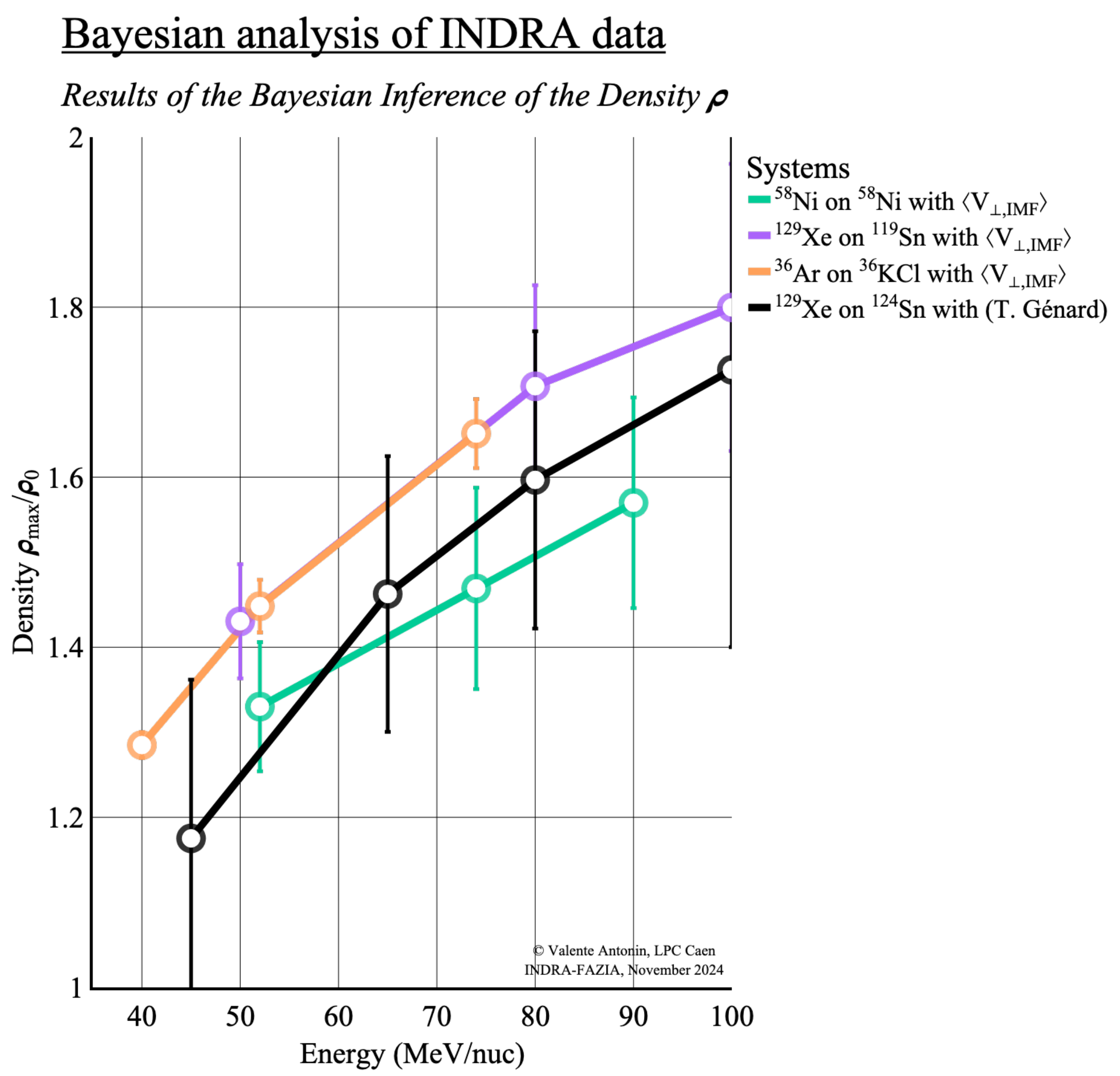

- Maximum density-sensitive selection of global observables ρ_{max}
- **Replicating and improving Tom's PhD Thesis results** (T. Génard 2023 PhD Thesis) with Bayesian inference.
- A conservative **estimate of the uncertainty is obtained at** $\sim 10\,\%$ **level based on experimental information**.
- ρ_{max} **reach** $1.8\rho_0$ **at** 100 **MeV/nucleon**.
- The mass hierarchy of the systems has to be investigated.

7. Contribution for the compression energy

Hypothesis : $$E_{comp} = \gamma \left(E_{cm} - E_{th} \right)$$

From the EOS : $$E_{comp}(\rho) = K_\infty \frac{(\rho - \rho_0)^2}{18\rho_0}$$

Results : $$\frac{\rho}{\rho_0} = 1 + \sqrt{\frac{\gamma(E_{cm} - E_{th})}{18K_\infty}}$$

as a linear form : $$\left(\frac{\rho}{\rho_0} - 1 \right)^2 \frac{1}{18} = \frac{\gamma}{K_\infty} \left(E_{cm} - E_{th} \right)$$

- We use a linear approach for the compression. We approximate the compression energy as a fraction of the energy available in the center of mass. γ **is the compression factor and E_{th} is a energy threshold.**
- We can plug the hypothetical formula into the expression of the EOS compression energy. We then deduce a functional of ρ and the energy available in the center of mass E_{cm}.
- We then reformulate this functional to get a linear form and fit the (γ, E_{th}) for a given systematic with (ρ, E_{cm})...

Results for the compression energy

Radial Energy Systematics

(B. Borderie et al, 2008, PPNP, 61, 2 551—601)

$$\gamma \sim 0.3 - 0.5$$
$$u(\gamma) \sim 20\,\%$$

Système	Notre Table			Borderie et al		
	γ	$u(\gamma)$	$\frac{u(\gamma)}{\gamma}$	γ	$u(\gamma)$	$\frac{u(\gamma)}{\gamma}$
$^{36}Ar + KCl$	0,52	0.17	33%	-	-	-
$^{58}Ni + ^{58}Ni$	0.31	0.05	16%	0.33	0.28	86%
$^{129}Xe + ^{119}Sn$	0.54	0.10	19%	0.38	0.30	78%
$^{197}Au + ^{197}Au$	-	-	-	0.43	0.09	21%
$^{36}Ar + ^{45}Sc$	-	-	-	0.47	0.05	11%
$^{84}Kr + ^{197}Au$	-	-	-	0.38	0.10	26%

$$E_{th} \sim 7\ MeV/nuc$$
$$u(E_{th}) \sim 10\,\%$$

Système	Notre Table			Borderie et al		
	E_{th} (MeV/A)	$u(E_{th})$	$\frac{u(E_{th})}{E_{th}}$	E_{th} (MeV/A)	$u(E_{th})$	$\frac{u(E_{th})}{E_{th}}$
$^{32}Ar + ^{32}KCl$	8.39	9.99	119%	-	-	-
$^{58}Ni + ^{58}Ni$	8.02	1.11	14%	5.40	4.58	85%
$^{129}Xe + ^{119}Sn$	7.97	0.41	5%	6.61	3.20	48%
$^{197}Au + ^{197}Au$	7.66	1.78	23%	5.27	2.81	53%
$^{36}Ar + ^{45}Sc$	-	-	-	3.27	1.82	56%
$^{84}Kr + ^{197}Au$	-	-	-	5.83	2.47	42%

From compression to density

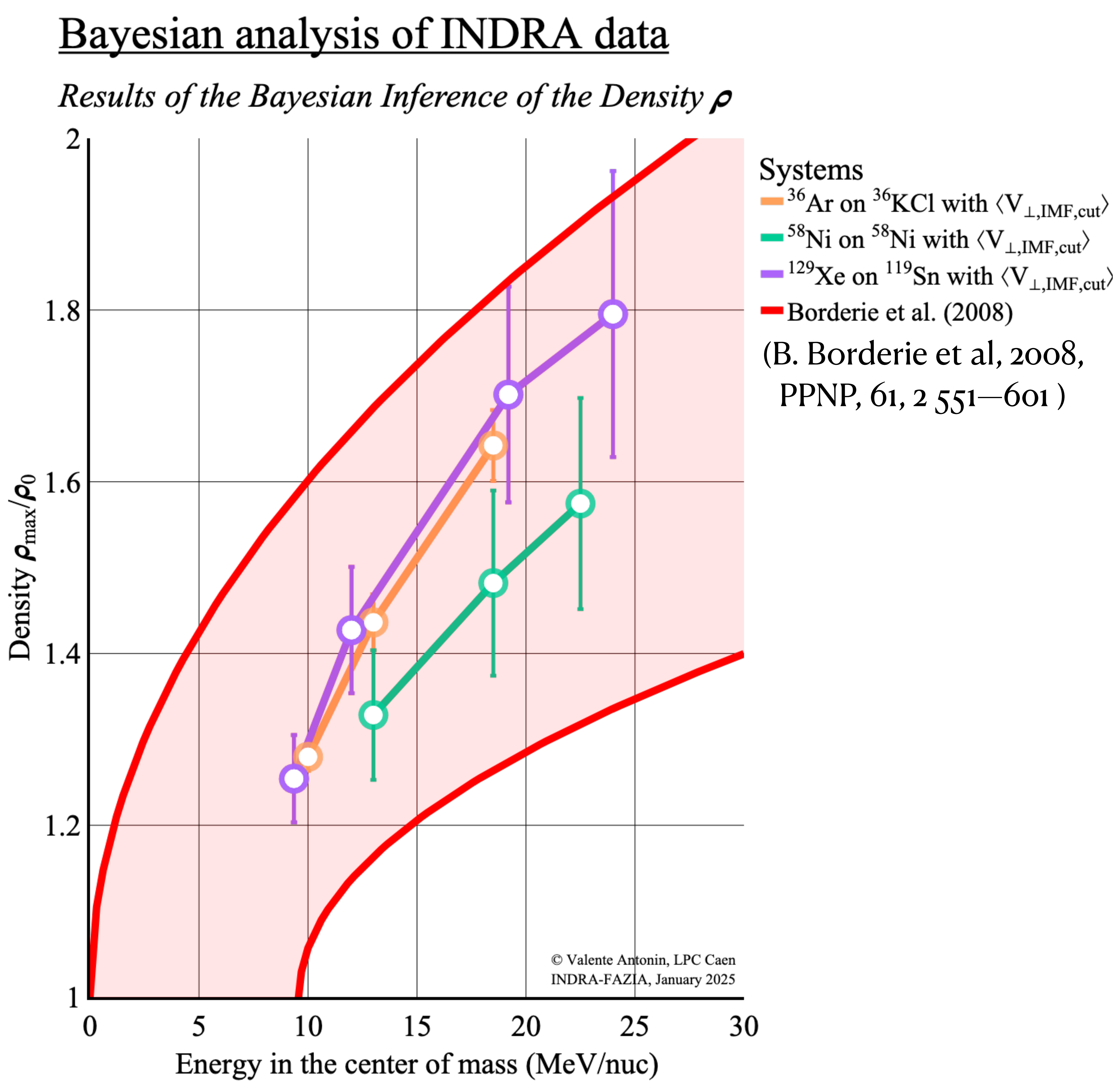

(B. Borderie et al, 2008, PPNP, 61, 2 551—601)

Système	Notre Table			Borderie et al		
	γ	$u(\gamma)$	$\frac{u(\gamma)}{\gamma}$	γ	$u(\gamma)$	$\frac{u(\gamma)}{\gamma}$
$^{36}Ar + KCl$	0,52	0.17	33%	-	-	-
$^{58}Ni + {}^{58}Ni$	0.31	0.05	16%	0.33	0.28	86%
$^{129}Xe + {}^{119}Sn$	0.54	0.10	19%	0.38	0.30	78%
$^{197}Au + {}^{197}Au$	-	-	-	0.43	0.09	21%
$^{36}Ar + {}^{45}Sc$	-	-	-	0.47	0.05	11%
$^{84}Kr + {}^{197}Au$	-	-	-	0.38	0.10	26%

- Our deduction extends the Borderie et al data results on the γ parameter. **And $\gamma = 0.3 - 0.5$ is coherent with Dominique DURAND's work where it is found** $\gamma = 0.4$.
- With the value of compression deduce with the Borderie's data, we can deduce the range of densities ρ in red. **Our calculations are consistent with the experimental data**.
- **We reach $1.8\rho_0 \sim 100$ MeV/nucleon.**

8. Perspectives

- Improvement of the *in-medium* nucleon nucleon cross section results with a bayesian inference and the use of HIPSE model.
- An exploration to study the Symmetry energy with INDRA Data is foreseen with $^{124,136}Xe/^{112,124}Sn$ at 32 and 45 MeV/Nucleon (fifth campaign).

Thanks for you for your attention !

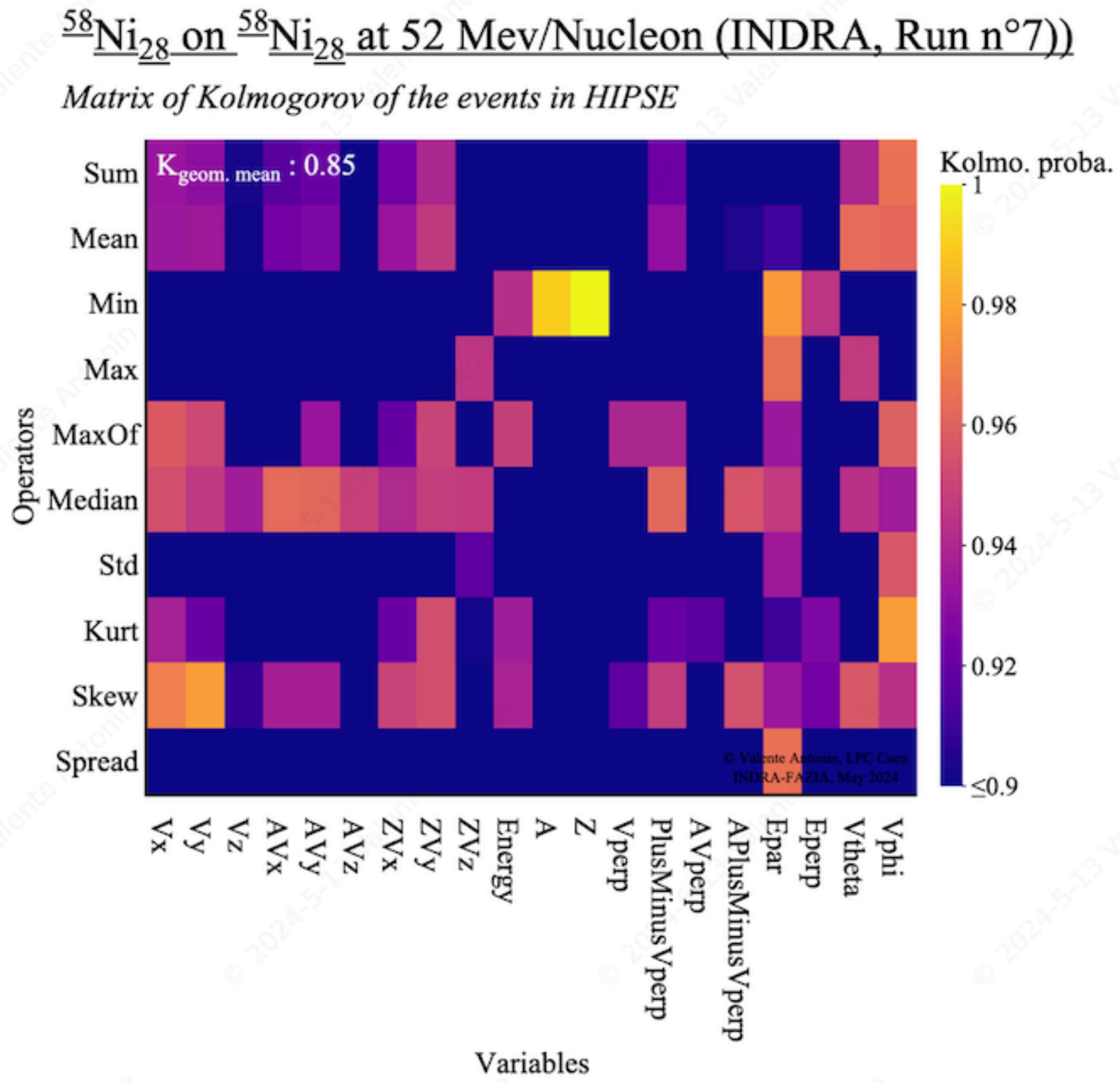

$^{58}Ni_{28}$ on $^{58}Ni_{28}$ at 52 Mev/Nucleon (INDRA, Run n°7))
Matrix of Kolmogorov of the events in HIPSE
$K_{geom. mean}$: 0.85
Kolmo. proba.
Operators
Sum
Mean
Min
Max
MaxOf
Median
Std
Kurt
Skew
Spread
Variables
Vx
Vy
Vz
AVx
AVy
AVz
ZVx
ZVy
ZVz
Energy
A
Z
Vperp
PlusMinusVperp
AVperp
APlusMinusVperp
Epar
Eperp
Vtheta
Vphi
1
0.98
0.96
0.94
0.92
≤0.9
© Valente Antonin, LPC Caen
INDRA-FAZIA, May 2024

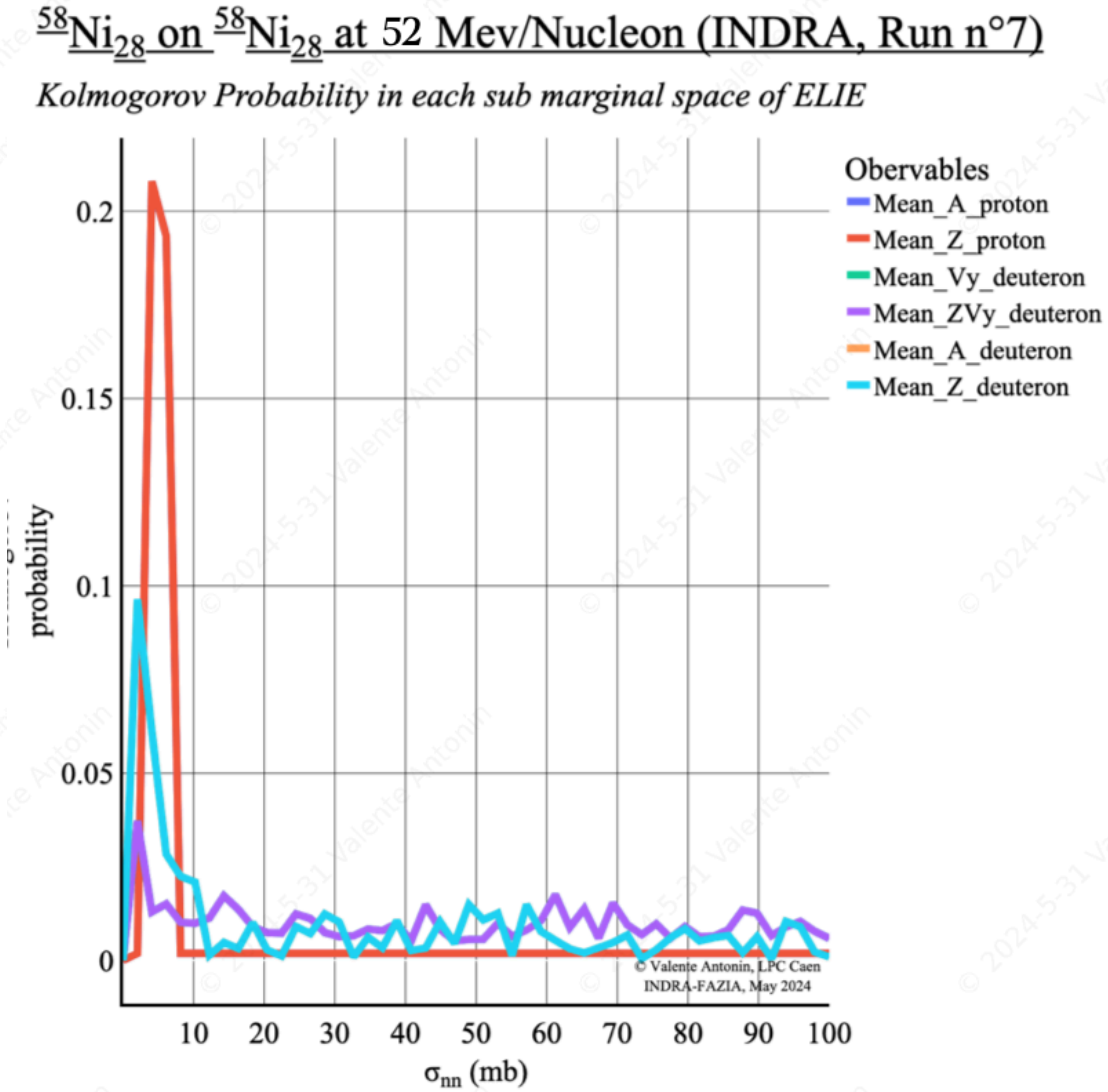

$^{58}Ni_{28}$ on $^{58}Ni_{28}$ at 52 Mev/Nucleon (INDRA, Run n°7)
Kolmogorov Probability in each sub marginal space of ELIE
probability
σ_{nn} (mb)
Obervables
Mean_A_proton
Mean_Z_proton
Mean_Vy_deuteron
Mean_ZVy_deuteron
Mean_A_deuteron
Mean_Z_deuteron
© Valente Antonin, LPC Caen
INDRA-FAZIA, May 2024

Bayesian analysis of INDRA data

Results of the Bayesian Inference of the Density ρ

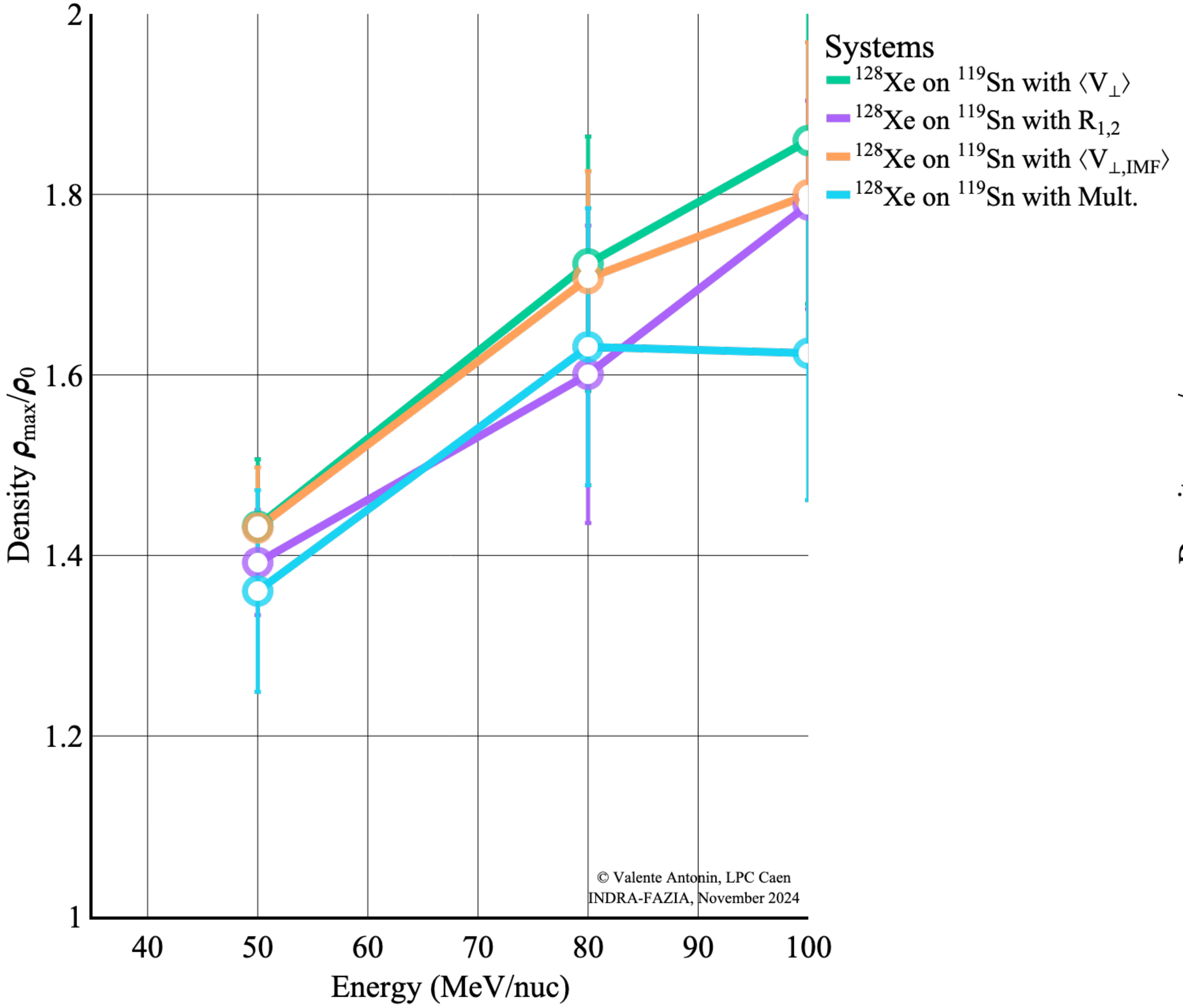

Bayesian analysis of INDRA data

Results of the Bayesian Inference of the Density ρ

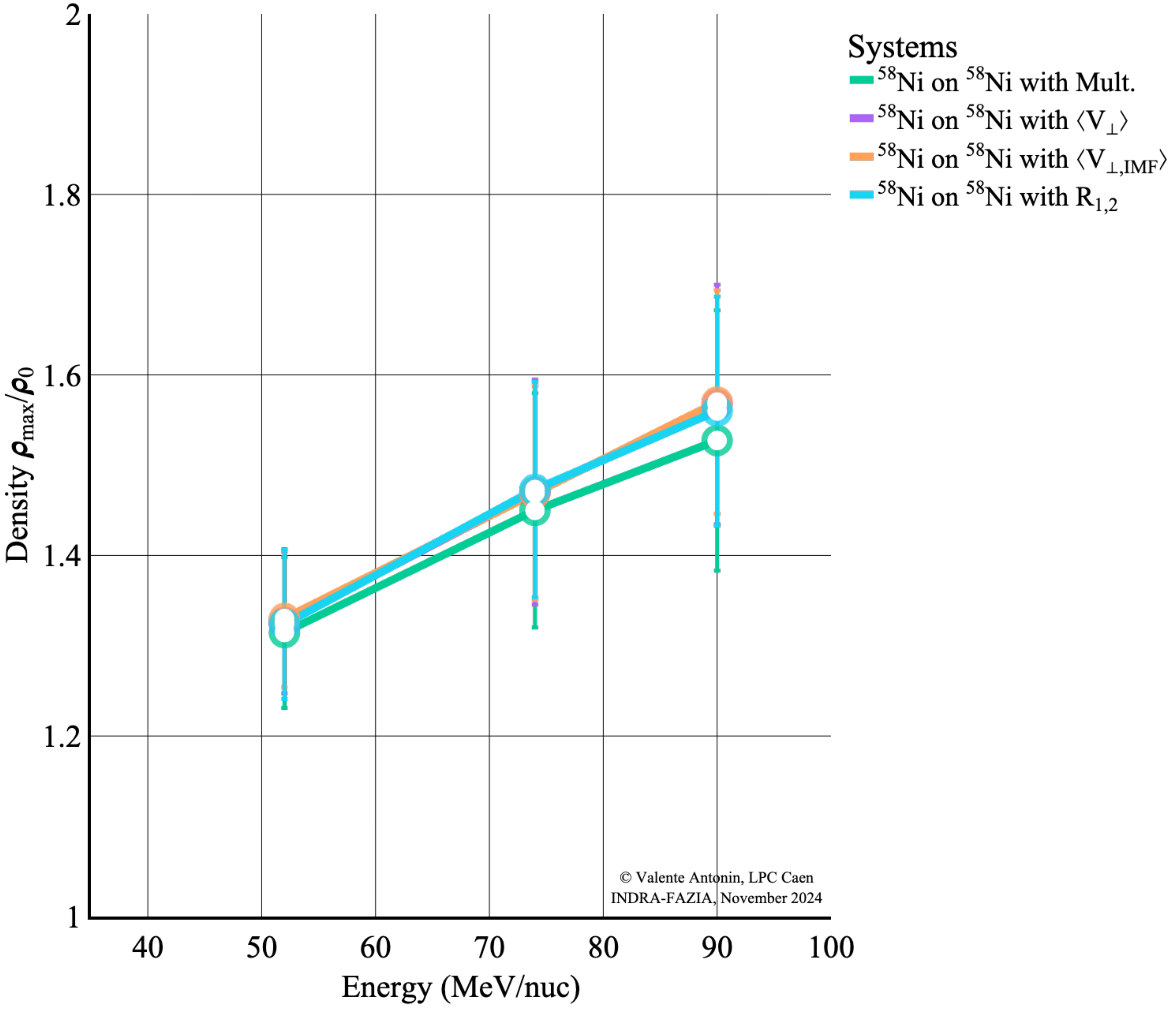

Bayesian analysis of INDRA data

Fits of the Density functionnal ρ with E_{cm}

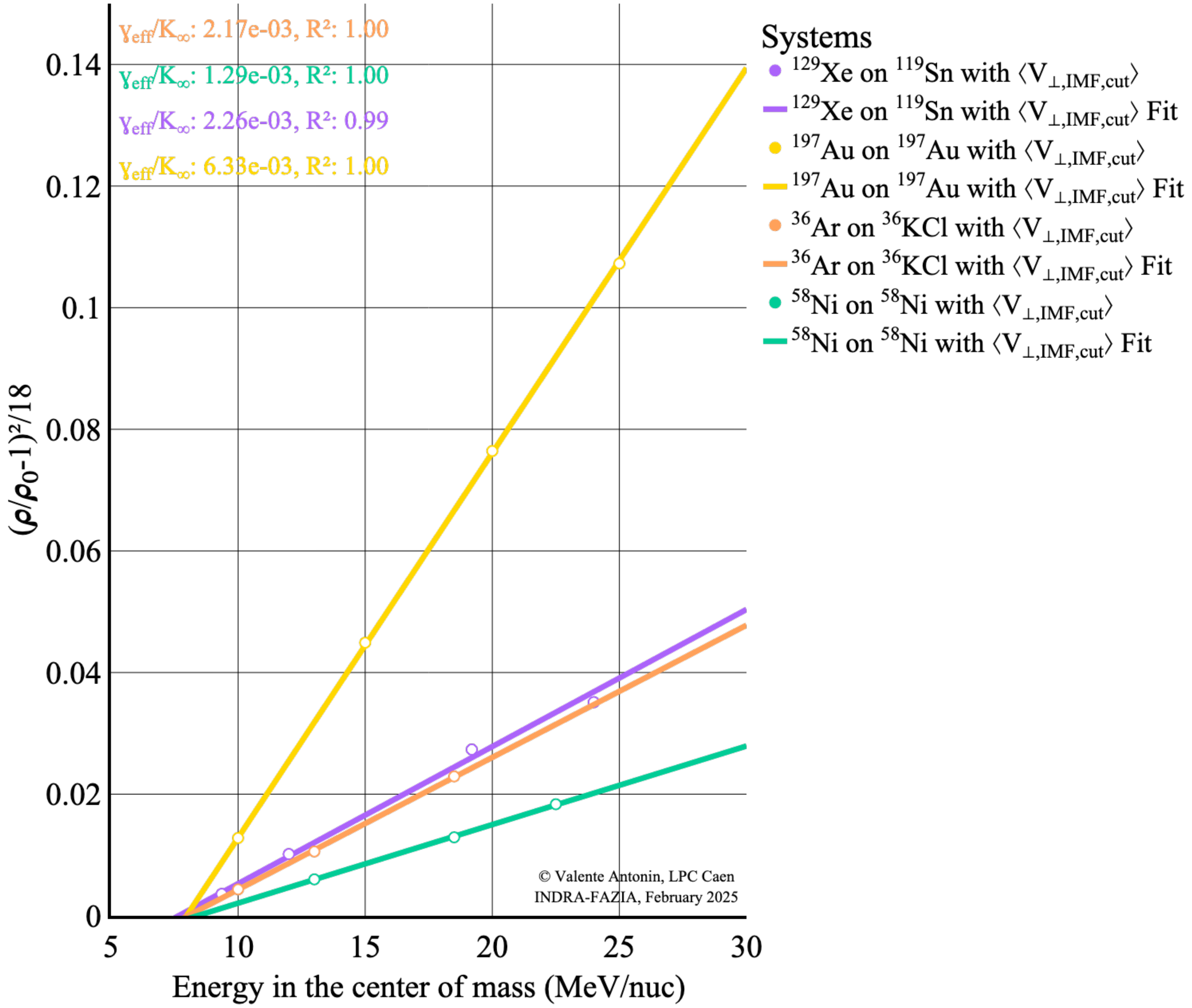

B. Borderie, M.F. Rivet / Progress in Particle and Nuclear Physics 61 (2008) 551–601

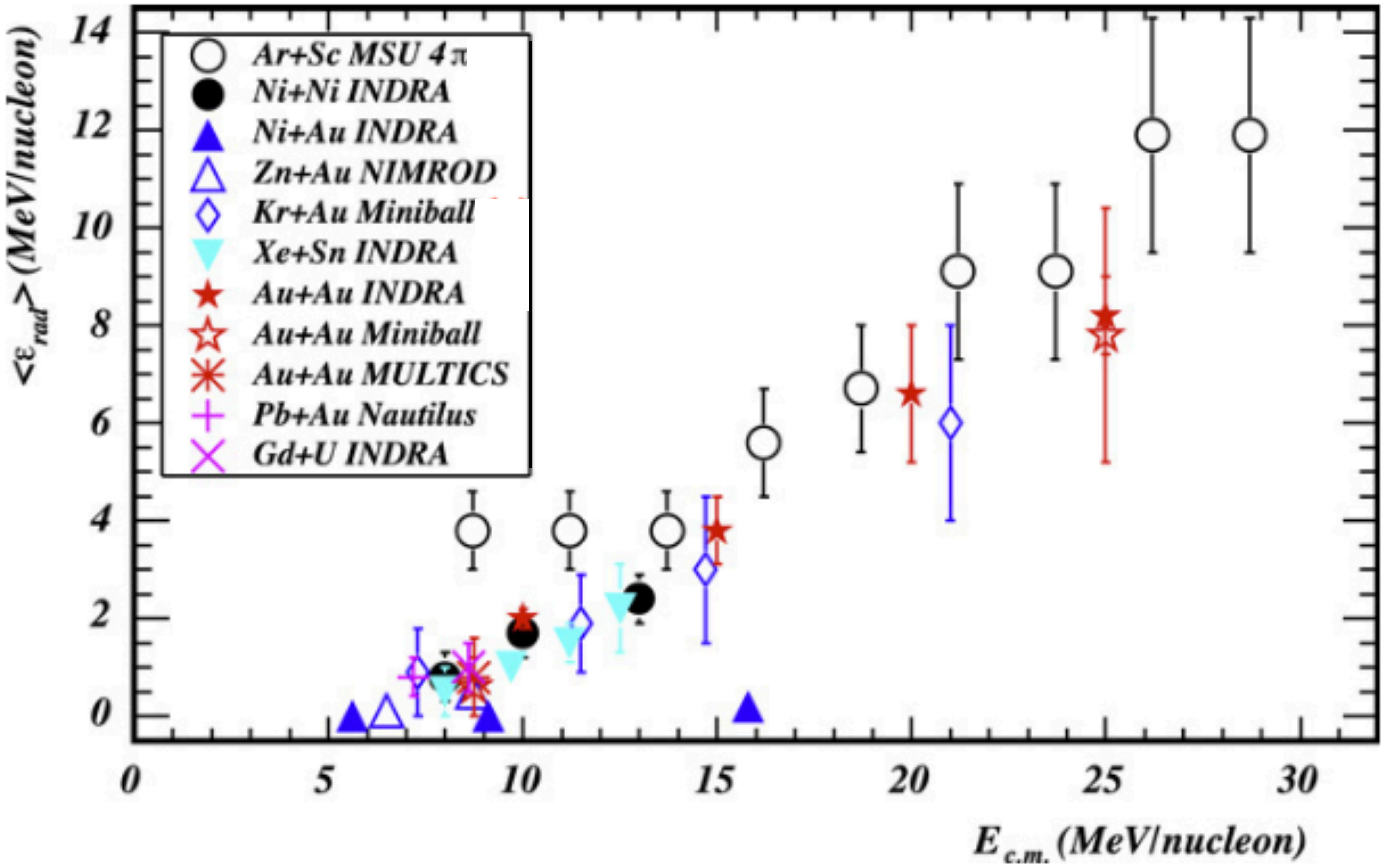

Bibliography

[1] Margueron JÉRÔME, Hoffmann Casali RUDINEY et Gulminelli FRANCESCA. "Equation of state for dense nucleonic matter from metamodeling. I. Foundational aspects". In : *Physical Review C* 97.025805 (2018).

[2] Olivier LOPEZ. "Critical review of isospin observables for the determination of the symmetry energy". In : sous la dir. de NUSYM. 2021.

[3] WG LYNCH et MB TSANG. "Decoding the density dependence of the nuclear symmetry energy". In : *Physics Letters B* 830 (2022), p. 137098.

[4] Maxime HENRI. "Étude des propriétés de transport dans et d'équilibration de la matière nucléaire dans le domaine des énergies de Fermi". Thèse de doct. Université Caen Normandie, 2018.

[5] G LEHAUT et al. "Study of nuclear stopping in central collisions at intermediate energies". In : *Physical Review Letters* 104.23 (2010), p. 232701.

[6] Coupland D D S, Lynch W. G et Tsang M. B. "Influence of transport variables on isospin transport ratios". In : *Physical Review C* 84.054603 (2011).

[7] Olivier LOPEZ. "Fragment production in nuclear collisions around Fermi energy ; Production de fragments dans les collisions nucleaires autour de l'energie de Fermi". In : (2014).

[8] Bernard Tamin DOMINIQUE DURAND Eric Sureau. 2001.

[9] Eric SURAUD. *L'équation d'état de la matière nucléaire*. Cours de l'école Joliot Curie, 1990.

[10] Philippe CHOMAZ et al. *Dynamics and Thermodynamics with nuclear degrees of freedom*. T. 30. 1. Springer Science & Business Media, 2007.

[11] JOËL POUTHAS. "Principes et techniques de la detection". In : *chez Ecole Internationale Joliot-Curie, Seignosse* (2008).

[12] JOEL POUTHAS et al. "INDRA, a 4π charged product detection array at GANIL". In : *Nuclear Instruments and Methods in Physics Research Section A : Accelerators, Spectrometers, Detectors and Associated Equipment* 357.2-3 (1995), p. 418-442.

[13] FAZIA COLLABORATION et al. "The FAZIA project in Europe : R&D phase". In : *The European Physical Journal A* 50 (2014), p. 1-20.

[14] E. LEGOUÉE. "Étude systématique de la dynamique et de la thermodynamique des systèmes nucléaires symétriques ou quasi-symétriques étudiés avec le multidétecteur INDRA par des méthodes probabilistes nouvelles". Theses. Université de Caen, oct. 2013. URL : https://theses.hal.science/tel-00881082.

[15] Stefano CARBONI et al. "Particle identification using the ΔE–E technique and pulse shape discrimination with the silicon detectors of the FAZIA project". In : *Nuclear Instruments and Methods in Physics Research Section A : Accelerators, Spectrometers, Detectors and Associated Equipment* 664.1 (2012), p. 251-263.

[16] S VALDRÉ et al. "The FAZIA setup : A review on the electronics and the mechanical mounting". In : *Nuclear Instruments and Methods in Physics Research Section A : Accelerators, Spectrometers, Detectors and Associated Equipment* 930 (2019), p. 27-36.

[17] G PASTORE et al. "Isotopic identification using Pulse Shape Analysis of current signals from silicon detectors : Recent results from the FAZIA collaboration". In : *Nuclear Instruments and Methods in Physics Research Section A : Accelerators, Spectrometers, Detectors and Associated Equipment* 860 (2017), p. 42-50.

[18] Diego D. GRUYER. "Aspects dynamiques de la désexcitation nucléaire : de la fission à la multifragmentation." Theses. Université de Caen-Basse Normandie, sept. 2014. URL : https://in2p3.hal.science/tel-01079916.

[19] Denis LACROIX, Aymeric VAN LAUWE et Dominique DURAND. "Event generator for nuclear collisions at intermediate energies". In : *Physical Review C—Nuclear Physics* 69.5 (2004), p. 054604.

[20] D DURAND. "An event generator for the study of nuclear collisions in the Fermi energy domain (I). Formalism and first applications". In : *Nuclear Physics A* 541.2 (1992), p. 266-294.

[21] Luciano G MORETTO. "Statistical emission of large fragments : A general theoretical approach". In : *Nuclear Physics A* 247.2 (1975), p. 211-230.

[22] Vincent MÉTIVIER. "Mécanismes de réaction et de dissipation de l'énergie dans les collisions symétriques noyau-noyau de 25 à 74 MeV/u : apport des mesures exclusives du multidétecteur INDRA". Thèse de doct. Caen, 1995.

[23] O Lopez et al. “Improving isotopic identification with INDRA Silicon–CsI (Tl) telescopes”. In : *Nuclear Instruments and Methods in Physics Research Section A : Accelerators, Spectrometers, Detectors and Associated Equipment* 884.034609 (2018), p. 140-149.

[24] R. J. Charity. “N-Z distributions of secondary fragments and the evaporation attractor line”. In : *Physical Review C* 54.2 (1998).

[25] R. J. Charity et al. “Emission of complex fragments from highly excited systems produced in 93Nb+9Be and 27Al reactions at E/A = 25.4 and 30.3 MeV”. In : *Nuclear Physics A* A476 (1988), p. 516-544.

[26] J Frankland et al. “Model independent reconstruction of impact parameter distributions for intermediate energy heavy ion collisions”. In : *Physical Review C* 104.034609 (2021).

[27] F Haddad et al. “Impact parameter determination in experimental analysis using a neural network”. In : *Physical Review C* 55.3 (1997).

[28] S Hochreiter. “Long Short-term Memory”. In : *Neural Computation MIT-Press* (1997).

[29] Ian Goodfellow. *Deep learning*. T. 196. MIT press, 2016.

[30] S Kox et al. “Trends of total reaction cross sections for heavy ion collisions in the intermediate energy range”. In : *Physical Review C* 35.5 (1987), p. 1678.

[31] Tom Genard. “Dynamique de production des clusters dans les collisions de Xe+ Sn entre 32 et 150 A MeV”. Thèse de doct. Normandie Université, 2023.

[32] B Borderie et MF Rivet. “Nuclear multifragmentation and phase transition for hot nuclei”. In : *Progress in Particle and Nuclear Physics* 61.2 (2008), p. 551-601.